Università degli Studi di Padova

Dipartimento di Biologia

Corso di Laurea Magistrale in Biotecnologie Industriali

Investigating the interplay between extracellular matrix and metabolic rewiring in sarcoma aggressiveness

Relatore: Prof. Andrea Rasola

Dipartimento di Scienze Biomediche

Controrelatrice: Prof.ssa Chiara Rampazzo

Dipartimento di Biologia

Laureanda: Francesca Sbuelz

Anno Accademico 2023/2024

INDEX

1. Abstract

The extracellular matrix (ECM) is one of the major structural components of the tumour microenvironment, and it is mainly composed of collagen molecules. During tumorigenesis the ECM undergoes a profound remodelling to sustain cancer cell aggressiveness. Nevertheless, the molecular mechanisms that orchestrate the ECM remodelling are largely unclear. Recent evidence suggests the existence of a link between the ECM composition and the metabolic state of cancer cells. Cancer cells rewire glutamine (Gln) metabolism to promote tumour progression and, Gln is a precursor of Proline, one of the most abundant amino acids found in collagens. My laboratory has previously shown that the mitochondrial chaperone TRAP1 is a master regulator of metabolic circuits in cancer cells, and cells lacking TRAP1 show lower collagen VI (col VI) levels. In the framework of my thesis, I investigated whether changes in amino acid metabolism sustain cancer cell tumorigenicity by tuning the ECM composition, and the role played by TRAP1 in this process. To this aim, I performed several i*n vitro* tumorigenic assays in cancer cells from an aggressive tumour of the peripheral nerve sheath (MPNST). I found that: i) Gln availability influences MPNST proliferation; ii) both TRAP1 and Col VI affect MPNST cell migration and invasion.

2. Introduction

2.1. The extracellular matrix

The extracellular matrix (ECM) is a highly dynamic structural meshwork that surrounds cells in metazoan organisms. By acting as a physical scaffold, the ECM allows cell organisation in tissues and organs. This three-dimensional (3D) structure exists as two different entities, which are intimately interconnected: i) the basement membrane (BM), which separates the epithelium from the surrounding stroma; ii) the interstitial matrix, which is located in the lamina propria, submucosa, and in the muscular and serosa layers (Pompili et al., 2021). The ECM continuously undergoes remodelling processes with changes in its components and features, thus contributing to a variety of biological processes both in physiological and pathological conditions (Theocharis et al., 2016). During my internship, I largely investigated the role(s) of an ECM component, collagen VI (COL VI) during tumorigenesis in a model of Malignant Peripheral Nerve Sheath Tumor (MPNST), and the interplay between tumor cell metabolism and ECM. For a better comprehension of the experimental work included in this thesis (see results, below), hereafter I start describing the main structural components of the ECM, the molecular mechanisms underlying ECM remodelling, and the main functions ascribed to the ECM, focusing on cancer. Then, I will discuss mitochondrial metabolic rewiring in cancer and its crosstalk with ECM components, as well as on the features that characterize MPNSTs.

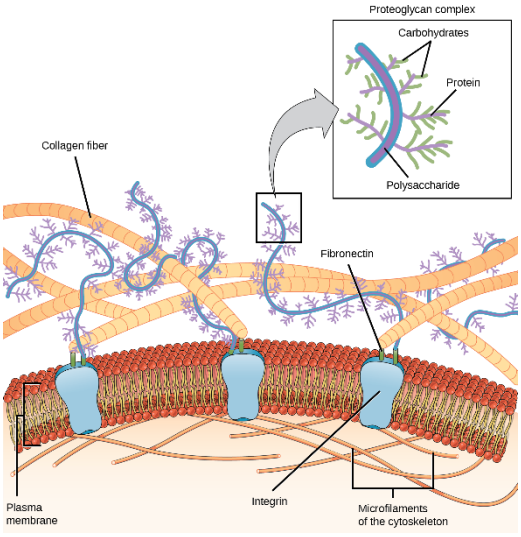

Figure 2.1. The ECM is a complex structural network. *OpenStax Biology.*

ECM structural components

Thanks to genome sequencing techniques and bioinformatic analyses, about 300 genes encoding ECM structural proteins have been identified. These genes can be grouped in three main categories: i) genes encoding collagen proteins; ii) genes encoding proteoglycans; iii) genes encoding glycoproteins (Naba, 2024).

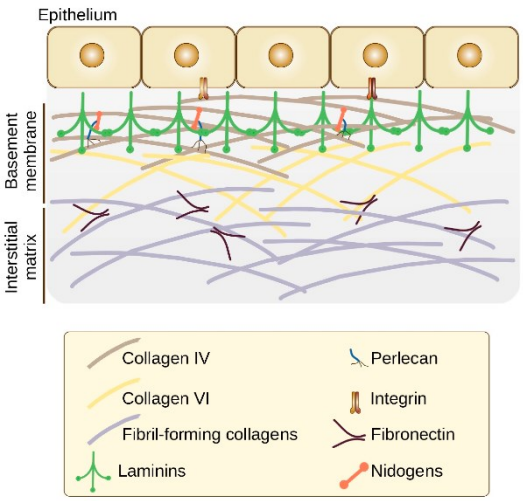

Figure 2.2. ECM organization in basement membrane and interstitial matrix. *Popova et al., 2022.*

With regard to the first category, 44 genes encoding collagen chains have been identified. After their synthesis, collagen chains undergo either homotrimeric or heterotrimeric assembly to give rise to 28 different collagen proteins. Even though collagen chains differ to some extent, they all consist of triple-helix motifs composed of glycine (Gly)-X-Y repeats, where the amino acids X and Y are commonly proline (Pro) and hydroxyproline (Hyp) residues. Collagen triple helices can further organize in supramolecular structures with specific geometric patterns that allow their subdivision in 4 main classes: i) fibril-forming collagens (I, II, III, V, XI, XXIV and XXVII); ii) Fibril-Associated Collagens with Interrupted Triple helices (FACITs; IX, XII, XIV, XVI, XIX, XX, XXI and XXII); iii) network-forming collagens (IV, VIII and X); iv) beaded collagens, such as collagen VI and VII, which are characterized by the presence of a "von Willebrand factor A" (VWA) domain in their modular structure.

COL VI is a well-established component of most interstitial matrices. Nevertheless, in some cases, COL VI forms a microfibrillar network associated to the basement membrane, or localizes in its close proximity. The anchoring to the BM mostly relies on the establishment of interactions with laminin proteins (see below, glycoprotein section) (Mak and Mei, 2017). From a structural point of view, COL VI consists of three α peptide chains, which are encoded by six different genes known as COL6A1, COL6A2, COL6A3, COL6A4, COL6A5 and COL6A6. Triple helices formed by α1, α2 and α3 chains are the most common COL VI structures found in animal tissues. Nevertheless, α3 chain can be replaced by α4 or α5, α6 chains in a tissue-specific manner. On the contrary, chains α1 and α2 are always included in COL VI triple helices. COL VI chains are synthetized in the ER-Golgi compartments, and before secretion, collagen VI monomers assemble into dimers and tetramers by lateral association. In the extracellular space, COL VI multimers form a network of "beaded microfilaments" (Castagnaro et al., 2021) which confer mechanical support to cells. COL VI also acts as a signalling molecule and provides either pro-survival or antiapoptotic stimuli to cells (Cescon et al., 2016: Cheng et al., 2011), and it is overexpressed in a variety of human cancers, including pancreatic (Owusu-Ansah et al., 2019), ovarian (Ho et al., 2021), lung (Duan et al., 2020) and breast (Iyengar et al., 2005) cancer. The contribution of COL VI to tumour development can be different depending on the stage of the disease, and on the type of cancer. In glioblastoma, COL VI promotes adhesion and spreading of cancer cells, thus enhancing tumour metastasis (Han et al., 1995). COL VI also elicits angiogenesis, while its genetic ablation causes functional defects of blood vessels (You et al., 2012).

Proteoglycans are composed of a core protein decorated by at least one covalently bound sulfated glycosaminoglycan (GAG) chain. Depending on the molecular size of the protein component, proteoglycans can be further divided into small proteoglycans (*e.g.* biglycan, decorin) and large proteoglycans of several hundred

kilodaltons (*e.g.* aggrecan, perlecan, versican) (Naba, Nature, 2024). Thanks to the physicochemical characteristics of the GAG portion of the molecule, proteoglycans provide hydration and swelling pressure to the tissue, allowing cells to withstand compressional forces (Buschmann and Grodzinsky, 1995; Takahashi et al., 2014).

Glycoproteins of the ECM consist of a peptide chain that is covalently linked to mono-, di-, oligo- or polysaccharides. This category includes the largest number of ECM structural components. For a better comprehension of the experiments that I carried out during my internship, I will focus on laminins and fibronectin. Laminins are primary constituents of the BM along with collagen IV (COL IV). Laminin molecules are heterotrimers composed of α, β, and γ chains. Sixteen trimeric isoforms have been described so far, and these isoforms vary in cell and tissue specificity (Halper, Progress in Heritable Soft Connective Tissue Disease, 2021). The main function of laminins is to act as a bridge between cells and a variety of ECM molecules. More specifically, laminins interact with integrin receptors of epithelial cells, connecting them with the basement membrane. Similarly to collagen molecules, laminins are involved in different stages of tumor progression, including neoplastic cell invasion and metastasis formation (De Arcangelis et al., 2001; Oikawa et al., 2011).
Fibronectin is a high molecular weight dimeric protein that is composed by type I, type II and type III repeating modules. Following its secretion in the extracellular space and interaction with integrins on the cell surface, fibronectin undergoes force-dependent conformational changes and formation of fibrils that contribute to the architecture of the ECM scaffold. Fibronectin expression is increased in many solid tumors, and it has been shown to guide cancer cell invasion (Gopal et al., 2017). In glioma, fibronectin cooperates with collagen I (COL I) to promote cancer cell proliferation and tumorigenicity (Zhong et al., 2021).

2.1.1. ECM functions

As mentioned above, ECM provides structural and mechanical support for tissue architecture. Nevertheless, further functions can be associated to the ECM. It is a reservoir of biomolecules (*e.g.*, growth factors, cytokines, etc) that can be released during ECM remodelling, binding to cell surface receptors and triggering specific signalling pathways (Gattazzo et al., 2014). The ECM is also involved in the mechanotransduction process, through which mechanical forces that generate in the extracellular space are transmitted to the cell. Mechanotransduction implies the assembly of focal adhesions complexes (FAs). The cascade of events starts with the binding of ECM proteins to integrin receptors, followed by their clusterization. The intracellular domains of integrins hence establish tight connections with actin microfilaments in the cytoskeleton via recruitment of adaptor proteins such as talin and vinculin. As a result, actin assembles in thicker bundles known as stress fibres, which undergo contraction via recruitment of non-muscular myosin molecules. The main effects downstream to mechanotransduction events include changes in the

expression of genes involved in cell proliferation, as well as in cell migration (Romani et al., 2021), a process that is characterized by the continuous assembly and disassembly of FAs. In agreement with the importance of these processes for neoplastic progression and invasiveness, integrins, as well as other FA components are upregulated in several types of aggressive cancers (Desgrosellier et al., 2010).

2.1.2. ECM remodelling in the tumoral context

The ECM is a highly dynamic structure. Its structural components undergo continuous remodelling both in physiological and pathological conditions. In the tumoral context, remodelling processes are exacerbated, and they underlie all the stages of the disease, while significantly hampering treatment attempts by sequestering chemotherapeutics. In light of this importance in neoplastic progression, the ECM deposition has recently been defined as a further hallmark of cancer (Socovich and Naba, 2019). One of the most prominent change in the ECM composition in solid tumors is a dramatic increase in the synthesis and deposition of collagen molecules. In the tumor microenvironment (TME) these processes are mainly ascribed to cancer-associated fibroblasts (CAFs), a heterogeneous population originated from fibroblasts, and to cancer cells. (Belhabib et al., 2021).

After their deposition, collagen molecules undergo crosslinking processes that are mediated by enzymes of the lysyl oxidase (LOX) family. The result of an increased collagen deposition and of an increased crosslinking among collagen fibres is a stiffening of the ECM, which can encapsulate the growing tumour mass. Hence, the ECM acts as a barrier to drug diffusion and nutritional supply, contributing to the establishment of a hypoxic TME that causes the activation of several pro-tumorigenic signalling pathways. During tumor development, the ECM is also continuously degraded. Key enzymes involved in the breakdown of the ECM components are the matrix metalloproteinases (MMPs). The latter are mainly secreted by fibroblasts, macrophages and neutrophils and can be classified into six groups: collagenases, gelatinases, stromelysins, matrilysins, membrane-type MMPs and other non-classified MMPs (Jabłońska-Trypuć et al., 2016). MMPs are synthesized as zymogens (*i.e.* inactive enzymes) and are in turn activated by proteolytic cleavage by plasmin and trypsin enzymes, as well as by further metalloproteinases. Activation and inhibition of these enzymes are regulated by

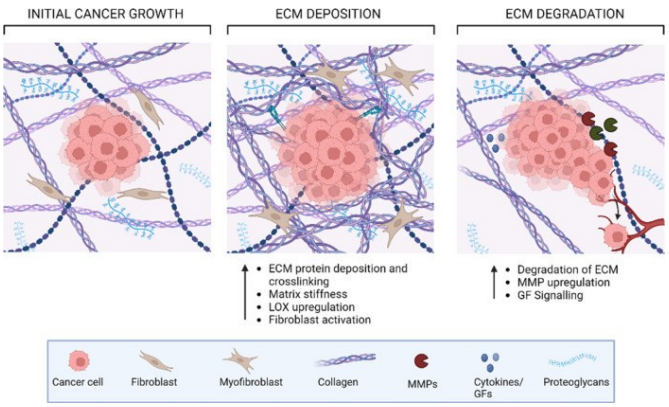

Figure 2.3. ECM remodelling in cancer. *Upadhyay et al., 2024.*

different factors. Inflammatory cytokines and growth factors increase the expression of MMPs, whereas corticosteroids and heparin are MMP inhibitors.
ECM degradation by MMPs is pivotal in cancer cell invasion and migration. The removal of specific components can indeed generate local paths through which cancer cell move. Nevertheless, this phenomenon is accompanied by an *ex novo* synthesis of the ECM macromolecules that act as anchoring sites for the moving cells.
In conclusion, the ECM in the tumour microenvironment undergoes a continuous remodelling that is required for the progression of the disease. Nevertheless, the molecular mechanisms promoting the ECM biosynthesis are yet to be identified.

2.2. Cancer metabolism

The TME is characterized by a reduced vascularization and by a limited supply of nutrients, including oxygen. In order to cope with such a hostile environment and with an increment in their proliferation rates, cancer cells rewire their metabolism in order to redirect building blocks to specific anabolic pathways to support neoplastic growth. Among others, cancer cells mainly rewire metabolic pathways related to glucose and amino acids.

2.2.1. Glucose metabolism

Glucose is taken up by cells through GLUTs transporters. In the cytosol, glucose is then converted into pyruvate by glycolytic enzymes. Oxidative decarboxylation then transforms pyruvate into acetyl-CoA, which enters the tricarboxylic acid cycle (TCA cycle) (Vander Heiden et al., 2009). Cancer cells display a marked increase in the uptake of glucose to boost glycolysis. Nevertheless, glucose-derived pyruvate is utilized to produce lactate instead of acetyl CoA, both in normoxic and hypoxic conditions. This boost of glycolysis independently of oxygen availability is known as the Warburg effect. Lactate produced by cancer cells is finally released in the extracellular space, where it lowers the pH levels and facilitates the MMP degrading activity. In this way, lactate contributes to cancer cell invasion, migration and metastasis formation (Bonuccelli et al., 2010).

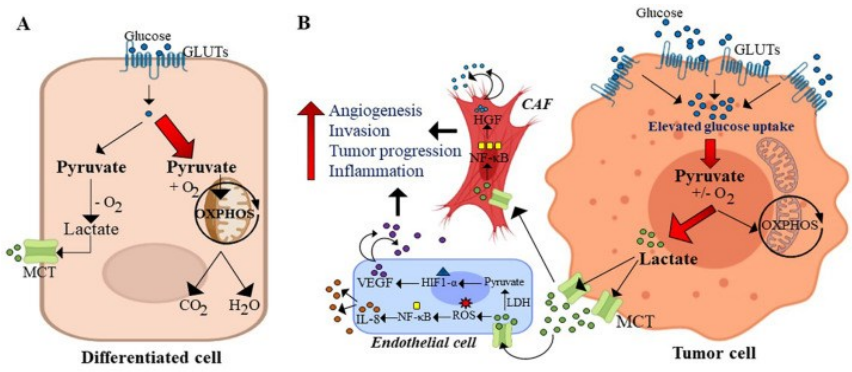

Figure 2.4. Representation of the Warburg effect in differentiated (A) and tumor cell (B). *Tyagi et al., 2021.*

Moreover, even though it is less efficient if compared to mitochondrial oxidative metabolism in terms of ATP production, glycolysis is upregulated by many cancer cells since it provides different precursors for biosynthetic pathways. Some glycolytic metabolites can indeed be diverted into other pathways to synthesize nucleotides, lipids, amino acids and other macromolecules required for cell proliferation.

2.2.2. Glutamine metabolism

In addition to glucose, cancer cells often increase the uptake and the use of various amino acids to support rapid proliferation rates. Serine and glycine are two critical amino acids that provide essential precursors to support nucleotide and protein synthesis. Serine and glycine metabolism is increased in cancer cells (Amelio et al., 2014).

Cancer cells also strictly depend on glutamine (Gln), which is a versatile substrate fuelling many anabolic pathways (Cruzat et al., 2018). As shown in Fig. 2.5. Gln is taken up by cells through the amino acid transporter SLC1A5, and it is then converted into glutamate (Glu) by glutaminase GLS. Glu, in turn, can be directed into different metabolic routes such as: i) the TCA cycle, after its conversion into α-ketoglutarate (which is catalysed by GLUD enzyme); ii) glutathione biosynthetic pathway; iii) proline (Pro) biosynthetic pathway. For a better comprehension of the set-up of the experiments included in this thesis, it is worth highlighting that Pro is one of the most abundant amino acid found in collagen molecules. Furthermore, Gln metabolic pathways are largely intertwined with those related to arginine (Arg), including Pro synthesis. As a corollary, Arg could complement promotion of collagen production under Gln deprivation. The high anabolic demand of cancer cells and the limited nutrient availability in the TME require a fine coordination of the bioenergetic circuits. As metabolic sensors, mitochondria play key roles in cellular adaptation to stress conditions. In the next paragraph, I will discuss some of the main mechanisms through which mitochondria support cancer cell growth.

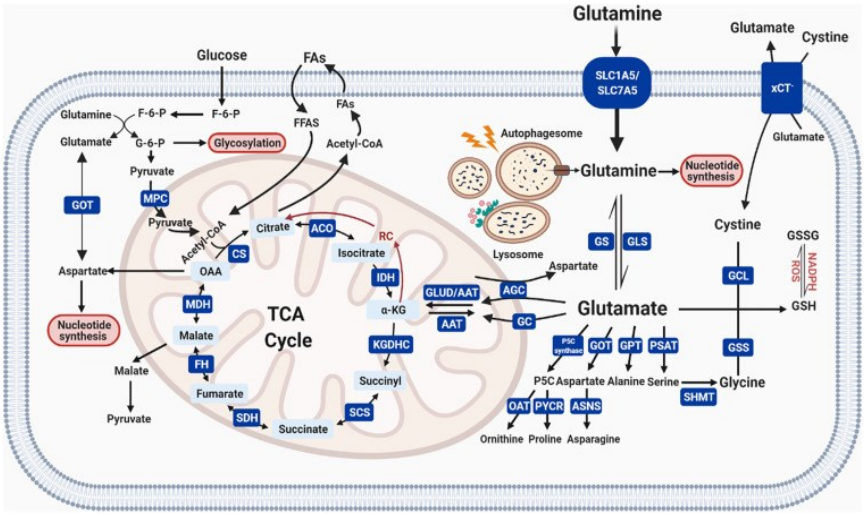

Figure 2.5. Schematic illustration of glutamine metabolism. *Shen et al., 2021.*

2.3. The role of mitochondria in cancer cell metabolism

The importance of mitochondrial metabolism for the tumorigenic process has been recognized for the first time with the identification of inactivating mutations in the genes encoding succinate dehydrogenase (SDH) and fumarate hydratase (FH), two main enzymes of the TCA cycle (Chandra and Singh, 2011). Loss of function mutations in SDH and FH respectively lead to the accumulation of succinate and fumarate that can act as oncometabolites. An increase in the intracellular levels of succinate leads to the stabilization of the transcription factor HIF-1α, which regulates the expression of various genes involved in angiogenesis, epithelial-mesenchymal transition (EMT), metastasis formation and metabolic rewiring (Keith et al., 2011). Furthermore, mitochondria can dynamically provide key metabolites to cancer cells for the synthesis of macromolecules required for tumor progression.

Through Gln catabolism mitochondria support Pro biosynthesis and thus collagen production.

The team leaded by Prof. Andrea Rasola and other research groups have identified the molecular chaperone TRAP1 as a master regulator of the metabolic functions in mitochondria of cancer cells; in the next paragraph, I will briefly discuss its molecular structure and its main roles.

2.4. The mitochondrial chaperone TRAP1

TRAP1 is the mitochondrial paralogue of the heat shock protein 90 (HSP90) family, and it has recently been identified as a key regulator of mitochondrial bioenergetics in cancer cells (Cannino et al., 2022). TRAP1 consists of two protomers; functional TRAP1 indeed acts as a homodimer and uses ATP to carry out its chaperone activity. Each protomer includes three domains: a N-terminal domain, a C-terminal domain (CTD) and a middle domain (M-domain). The N-terminal domain binds the

ATP, and it is responsible for its hydrolysis, whereas CTD provides the dimerization interface to form the homodimer, and the M-domain contains a pocket for the chaperone substrates (also known as client proteins). During the ATPase cycle, TRAP1 undergoes several conformational changes, which are summarized in figure 2.6 (see below). Briefly, after the binding of ATP molecules to the N-termini, TRAP1 assumes a closed asymmetrical conformation. At this point, hydrolysis of the ATP molecules provides the energy required for client remodelling (Masgras et al., 2017). The two ADP-bound protomers assume a closed conformation. Finally, the release of ADP molecules allows TRAP1 to return to its open conformation (also known as *apo* conformation).

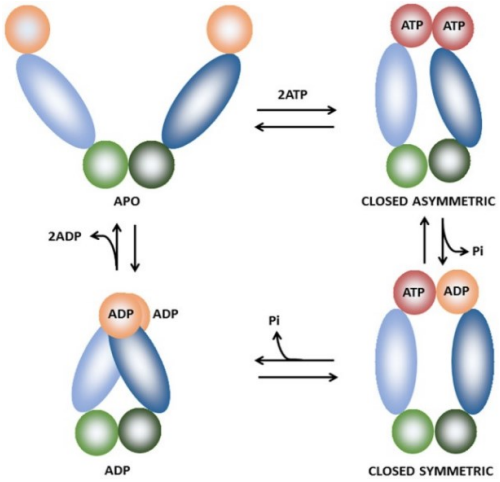

Figure 2.6. Representation of TRAP1 conformational changes. *Masgras et al., 2017.*

In physiological conditions, TRAP1 acts as an antioxidant molecule (Montesano et al., 2007). Accordingly, a reduced TRAP1 activity has been associated to an increase in ROS levels, and this has been linked to several disorders, such as Parkinson's disease (Butler et al., 2012).

TRAP1 has also been found to be overexpressed in a variety of cancer types (Rasola et al., 2014), and a direct correlation between TRAP1 expression levels and malignant progression has been observed (Gao et al., 2012). TRAP1 contributes to the switch toward aerobic glycolysis over mitochondrial oxidative metabolism in two ways: i) by downregulating the cytochrome oxidase, the complex IV of the respiratory chain (Yoshida et al., 2013); ii) by inhibiting the SDH, the complex II of the respiratory chain (Sciacovelli et al., 2013). The inhibition of SDH by TRAP1 leads to an increase in the intracellular levels of succinate. This, as discussed above, contributes to the stabilization of HIF-1α, with the consequent establishment of pseudohypoxic conditions (*i.e.,* induction of the HIF1α-dependent transcription program independently of hypoxia) and activation of pro-tumorigenic signalling pathways, which stimulate invasiveness, angiogenesis and a further metabolic rewiring of cancer cells (Semenza et al., 2013). In cancer cells, TRAP1 can also inhibit the opening of the permeability transition pore (PTP), a Ca^{2+}-activated

mitochondrial megachannel, hence antagonizing PTP-dependent mitochondrial depolarization and preventing cell death (Cannino et al., 2022).

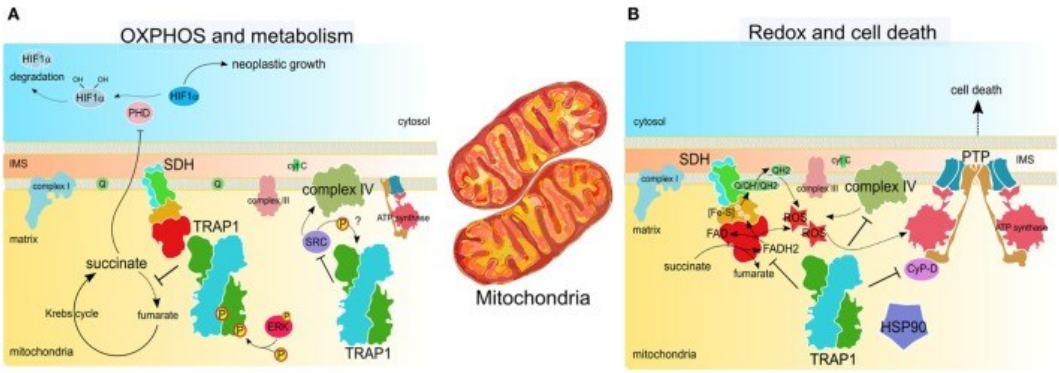

Figure 2.7. TRAP1 activity in cancer cells. *Masgras et al., 2017.*

Mass spectrometry analyses recently performed in the lab of Prof. Rasola have identified further TRAP1 interacting partners, including several enzymes involved in the amino acid metabolism and, in particular, in the biosynthesis of Pro (namely GLS1 and ALDH18A1) (see figure 2.8). These results suggest a much wider role for TRAP1 in the coordination of the metabolic routines of cancer cells, which could reverberate on collagen biosynthesis and therefore on the invasive capability of cancer cells.

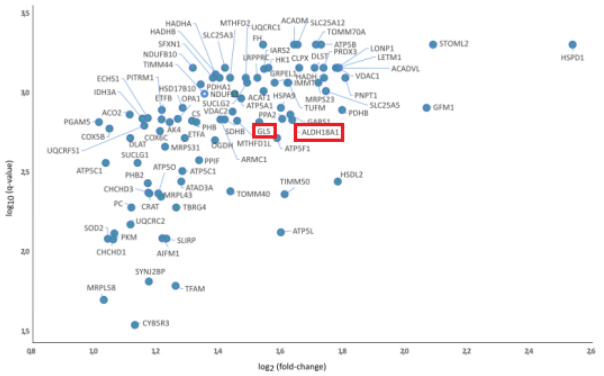

Figure 2.8. NanoLCMS/MS mass spectrometry analysis of TRAP1 interactors from U87 cells. *Image modified from Cannino et al., 2022.*

2.5. Crosstalk between ECM and metabolism

As discussed up to now, both remodelling of the ECM and rearrangement in the main metabolic circuits of cancer cells are pivotal to tumour progression, but any potential link between the two processes remained unexplored for many years. Recently, the discovery that mechanotransduction events can impact on cell proliferation, a process which requires metabolism of nutrients for fueling both bioenergetic and biosynthetic needs of neoplastic cells, has allowed to identify the cell microenvironment as a main regulator of cell metabolism (Romani et al., 2021).

The cell microenvironment and in particular the mechanical properties of the ECM can regulate cell metabolism in multiple ways. When placed on a stiff ECM, cells remodel their cytoskeleton and generate stress fibres. The latter have been shown to sequester a variety of glycolytic enzymes, hence protecting them from proteasomal degradation and leading to an increase in the glycolytic flux (Romani et al., 2021). The glucose transporter GLUT4 can also be upregulated by

mechanical cues. Insulin stimulation of skeletal muscle and adipose cells induce the translocation of GLUT4 from intracellular vesicle to the plasma membrane. This process occurs either thanks to the activation of vesicle trafficking by PI3K signalling or by the increased docking of vesicles in the plasma membrane enhanced by actin remodelling mediated the formation of FAs (Jaldin-Fincati et al., 2017).

Mechanical inputs from ECM can also regulate mitochondrial metabolic pathways, such as the Pro biosynthetic pathway. On a stiff ECM, kindlin 2, a protein which generally localizes at FAs (Guo et al., 2019), can also accumulate in mitochondria. Here, it interacts with PYCR1, a key enzyme involved in Pro synthesis, increasing its stability and activity. As consequence, cells on a stiff ECM have increased PYCR1 levels, increased Pro synthesis and cell proliferation (Guo et al., 2019). Since Pro is one of the most abundant amino acids found in collagens, it is worth noting that this mechanism could reinforce the collagen production, hence leading to the establishment of feedforward mechanism that would drastically increase the ECM stiffness. In agreement, a decrease in the expression levels of PYCR1 and, as a consequence, in the level of Pro, correlates with a significant reduction in collagen levels in the ECM and in tumor growth (Guo et al., 2019; Guo et al., 2020).

The aforementioned links between the mechanical properties of the ECM and cell metabolism shape the tumor milieu. Nevertheless, cell metabolism can, in turn, support the assembly of a pro-tumorigenic ECM and promote tumor progression. An example of this crosstalk is provided by the prolyl hydroxylase (PH) enzyme family. In order to hydroxylate Pro residues on their target peptides, PHs require α-ketoglutarate as a cosubstrate. Among others, PHs (specifically PH4) are responsible for the hydroxylation of collagen molecules. Therefore, it is plausible that alterations in the intracellular levels of α-ketoglutarate could hamper the maturation of collagens, thus reducing stiffness of the ECM. Recent evidences also suggest that Gln metabolism could be involved in controlling ECM architecture. Indeed, in cancer associated fibroblasts (CAFs), Gln is redirected to Pro biosynthesis instead of being funnelled into other anabolic pathways, in order to support the production of COL I and COL VI (Kay et al., 2022).

Preliminary isotope-based flux analyses performed in the lab leaded by Prof Andrea Rasola have shown that, likewise CAFs, cancer cells preferentially use Gln to derive Pro (Fig. 2.9).

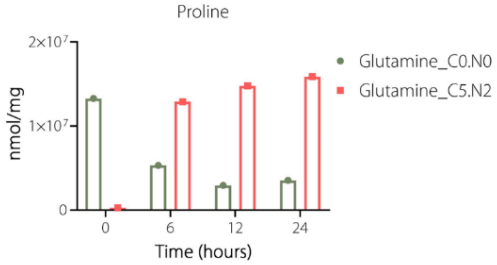

Figure 2.9. Pilot mass spectrometry flux analyses of intracellular metabolites based on the use of isotope-labelled Gln indicate that Gln is promptly taken up by cells and rapidly converted into Pro.

Although a direct connection is yet to be investigated, most likely this Gln-derived Pro is then directed to the biosynthesis of COL VI, since the levels of COL VI as shown in figure 2.10 (below) increase overtime when cancer cells are grown in extra-physiological amounts of Gln, and decrease under Gln deprivation (Fig. 2.10).

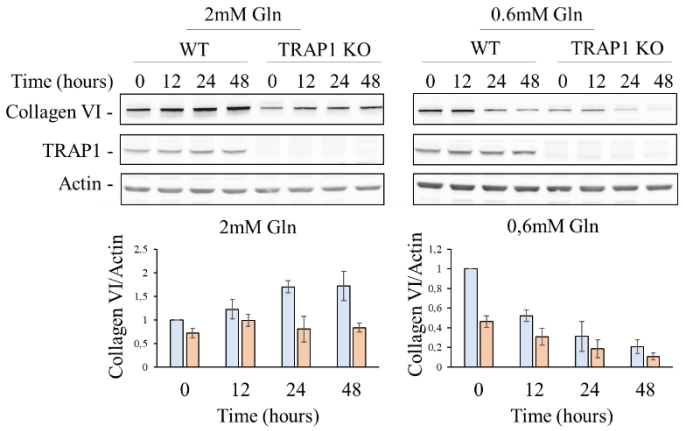

Figure 2.10. Western Blotting (WB) analyses show that collagen VI accumulates in MPNST cells cultured in high concentrations of Gln, while its levels decrease following Gln starvation.

As a further confirmation of the involvement of mitochondria in the regulation of metabolic pathways, lower COL VI protein levels have been observed in cells lacking TRAP1, if compared to those expressing TRAP1 (Fig. 2.10).

Nevertheless, the molecular mechanisms that underlie the interplay between cancer cell metabolism and ECM, as well as the role(s) played by COL VI in tumour development remain largely unexplored. During my internship, I focused on the set up of experiments aimed at testing how cancer cell tumorigenic properties could change depending on Gln availability and COL VI expression.

Experiments included in this thesis, as well as flux analyses and WB assays, have been performed by taking advantage of a mouse cancer cell line (sMPNST cells, see Materials and Methods), which derives from a malignant soft tissue sarcoma originating from peripheral nerves (termed Malignant Peripheral Nerve Sheath Tumor and hereafter referred as to MPNST). The three sMPNST cell lines (SCR, TRAP1 KO and COL VI KO) used in this thesis have been generated by taking advantage of the CRISPR/CAS9 genome editing technology (Fig. 2.11). In the next paragraph, I will discuss the main genetic alterations underlying MPNST development and its main histological features.

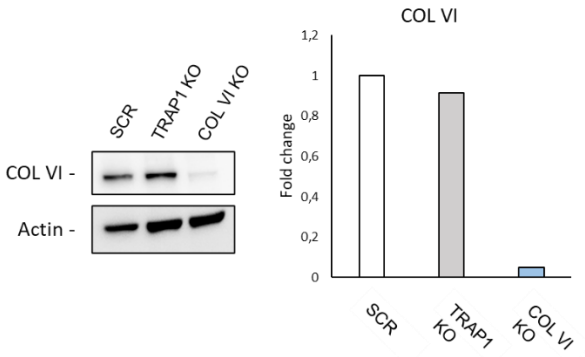

Figure 2.11. Western Blotting (WB) analysis validate the occurrence of the knock-down event and so the generation of COL VI KO sMPNST cell line.

2.6. Neurofibromatosis type 1 and MPNST

MPNST is a highly aggressive cancer type that develops either sporadically (Watson et al., 2017) or in patients affected by the tumor predisposing genetic syndrome Neurofibromatosis type 1 (NF1).

Briefly, NF1 is an autosomal dominant disorder with a incidence of 1/3000 individuals (Evans et al., 2010), and it is characterized by a wide range of variable clinical manifestations which include: i) abnormalities in the skin pigmentation, such as café-au-lait macules (CALMs) and freckles; ii) bone dysplasia, which is mainly due to a decreased bone mineral density; iii) iris hamartomas, known as Lisch nodules; iv) hypertension and other cardiovascular anomalies; v) alterations in cognition (Friedman et al., 2002). NF1 results from heterozygous inactivating mutations in the *Nf1* gene encoding a Ras GTPase activating protein (Ras-GAP) called neurofibromin, which acts as negative regulator of the Ras oncogene (DeClue et al., 1991; Abramowicz et al., 2014). In particular, neurofibromin accelerates the inactivation of Ras, by promoting the conversion of active Ras to the inactive GDP-bound form. Loss of neurofibromin hence leads to the hyperactivation of Ras, and of two downstream signalling pathways the PI3 kinase/Akt/mTOR and Raf/MEK/ERK pathways (see figure 2.12), predisposing patients to tumour development.

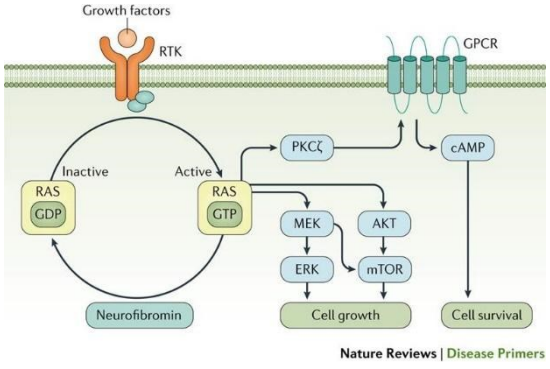

Figure 2.12. Neurofibromin signalling pathway. *Gutmann et al., 2017.*

Biallelic inactivation of *Nf1* in Schwann cells disrupts neurofibromin functions, worsening clinical conditions of NF1 patients and leading to the development of plexiform neurofibromas (Kluwe et al., 1999; Laycock-van Spyk et al., 2011). Even though they are extremely large in size, neurofibromas are benign tumours.

Nevertheless, 10% of neurofibromas undergoes transformation and gives rise to MPNSTs, if mutations in further oncogenes or oncosuppressors (*e.g. TP53, Pten, Suz12*) occur (Lee et al., 2014; Brohl et al., 2017). Currently, no cure is available for MPNSTs, and surgical excision is impeded by the large size of tumor mass and by cancer tendency to invade perineural tissues. Hence, prognosis for patients remains dismal (Uusitalo et al., 2016).

From a structural point of view, MPNSTs are characterized by a highly stiff ECM, which can account for up the 70% of tumour dry weight. Several evidences suggest COL VI to be one of the main components of the stiff ECM in MPNSTs. Nevertheless, the ECM composition, the molecular mechanism supporting its biosynthesis, and the role played by COL VI in MPNST development are yet to be explored.

3. Aim of the project

While the genetic signature of MPNSTs has largely been characterized, their metabolic profile and the contribution of the ECM to the progression of the disease are unknown. Exploring the bioenergetic features of MPNST, as well as assessing the composition of the ECM, is of most importance to identify new targetable factors for the design of valid therapeutic approaches, urgently needed to treat these aggressive sarcomas.

Preliminary data from the lab leaded by Prof Andrea Rasola suggest the existence of a link between amino acid metabolism and the biosynthesis of collagen VI. Therefore, during my internship, I first aimed at assessing the contribution of both Gln and COL VI to MPNST cell tumorigenicity.

Several enzymes involved in Gln metabolism have recently been identified as TRAP1 interacting partners. Hence, in the framework of my thesis, I also aimed at expanding our current knowledge about the role played by mitochondria in supporting MPNST growth. To achieve the aforementioned objectives, I took advantage of three sMPNST cell lines, namely SCR, TRAP1 KO and COL VI KO cells, and I set up several tumorigenic assays by growing cells in different Gln concentrations. For a better description of the experimental procedures implemented in this thesis project, see the next paragraphs (materials and methods, and results, below).

4. Materials and methods

4.1. Chemicals and plastics for cell cultures

Dulbecco's Modified Eagle's Medium - DMEM (4.5g/L D-glucose without sodium pyruvate and L-glutamine) (Gibco, Cat. No. 11960044); Dulbecco's Phosphate Buffered Saline (PBS) modified, without calcium chloride and magnesium chloride (Sigma-Aldrich, Cat. No. D8537); SILAC DMEM Flex Media (without D-glucose, L-glutamine, L-lysine, L-arginine, sodium pyruvate and phenol red) (Gibco, Cat. No. A2493901); Penicillin/Streptomycin (pen/strep) (10000 units/mL of penicillin; 10000 µg/ml of streptomycin) (Gibco, Cat. No. 15140122); Dialyzed Fetal Bovine Serum (dFBS) (Gibco, Cat. No. 26400044); Sodium pyruvate (Na^+/pyr) (Gibco, Cat. No. 11360070); L-Glutamine (Gln) (Gibco, Cat. No. 25030024); L-Lysine monohydrochloride (Lys) (Sigma, Cat. No. L5626); L-Arginine monohydrochloride (Arg) (Sigma, Cat. No. A5131); Glucose (Sigma, Cat. No. G7528); 0.05% and 0.25% Trypsin-EDTA solutions (Gibco, Cat. No. 25300054 or 25200056); Cultrex 3-D Culture Matrix Laminin I (R&D systems, Cat. No. 344600501); Collagen I (bovine) (Gibco, Cat. No. A10644-01); Fibronectin from bovine plasma (Sigma, Cat. No. F1141); Matrigel ® Growth Factor Reduced Basement Membrane Matrix (Corning, Cat. No. 356231); Low melting agarose (Promega, Cat. No. V2111); Crystal Violet (Fluka, Cat. No. 6113525G); Paraformaldehyde (Electron Microscopy Sciences, Cat.No. 15710); Triton X-100 (Sigma, Cat. No. 9036195); DAPI (Sigma, Cat. No. D95425MG); Phalloidin (Sigma, Cat.No. P1951).

CellCarrier Spheroid ULA 96-well Microplates (Revvity, Cat. No. 6055330); 24-Well Cell Culture Inserts with PET membranes (pore size: 8.0µm) (cell QART®, Cat. No. 9328012); RAL Diff-Quik™ kit (RAL DIAGNOSTICS, Cat. No. 720555-0000).

Medium used:

DMEM supplemented with 10% dFBS, 2mM glutamine, 1% pen/strep and 1mM Na^+/pyr. SILAC DMEM Flex Media supplemented with 10% dFBS, 2 mM Gln, 0.06 mM Arg, 0.8 mM Lys, 1% pen/strep, 1 mM Na^+/pyr, 25 mM glucose. SILAC DMEM Flex Media supplemented with 10% dFBS, 0.6 mM Gln, 0.06 mM Arg, 0.8 mM Lys, 1% pen/strep, 1 mM Na^+/py, 25 mM glucose. SILAC DMEM Flex Media supplemented with 0.05% dFBS, 2 mM Gln, 0.06 mM Arg, 0.8 mM Lys, 1% pen/strep, 1 mM Na^+/pyr, 25 mM glucose (used for Transwell assay). SILAC DMEM Flex Media supplemented with 0.05% dFBS, 0.6 mM Gln, 0.06 mM Arg, 0.8 mM Lys, 1% pen/strep, 1 mM Na^+/pyr, 25 mM glucose (used for Transwell assay). SILAC DMEM Flex Media supplemented with 1% dFBS, 2 mM Gln, 0.06 mM Arg, 0.8 mM Lys, 1% pen/strep, 1 mM Na^+/pyr, 25 mM glucose (used for spheroids culture). SILAC DMEM Flex Media supplemented with 1% dFBS, 0.6

mM Gln, 0.06 mM Arg, 0.8 mM Lys, 1% pen/strep, 1 mM Na^+/pyr, 25 mM glucose (used for spheroids culture).

4.2. sMPNST cell line and culture conditions

sMPNST cell line (kindly provided by Dr. Lu Q. Le, University of Texas Southwestern Medical Center, Dallas, TX) was established from Nf1- and p53-deficient skin precursors (SKP) (Le et al., 2009). Hence, CRISPR CAS9 genome editing was used to generate sMPNST cell lines lacking either TRAP1 or Collagen VI (COLVI) expression (hereafter referred to as TRAP1 KO and COLVI KO cell lines). A small guide RNA targeting EGFP (sgEGFP) was also used to generate a sMPNST cell line to serve as a control (hereafter referred to as SCR sMPNST cells).

sMPNST cells were maintained in DMEM supplemented with 10% dFBS, 2 mM glutamine, 1% pen/strep, 1 mM Na^+/pyr at 37°C in a humidified atmosphere with 5% CO_2, and regularly split before reaching 70-80% of confluence.

4.3. Proliferation assays

Cell proliferation rates of SCR (see Materials and methods), TRAP1 KO and COL VI KO sMPNST cells grown with media supplemented with either 0.6 mM or 2 mM Gln were assessed by performing the Crystal Violet assay. Briefly, $5x10^4$ sMPNST cells were seeded in SILAC DMEM medium supplemented with 10% dFBS, 2 mM Gln and 0.06 mM Arg on 12-well plates. At about 5-6 hours post-seeding, SILAC DMEM medium was replaced with SILAC media containing either low or high Gln, and 0.06 mM Arg. This was considered as the time zero for the proliferation assay, and sMPNST cell growth was monitored on a daily basis up to 5 days. Since the Crystal Violet assay implies cytological staining procedures, 5 different 12-well plates were prepared, one for each timepoint (0-, 24-, 48-, 72- and 96-hours). Every 24 hours, sMPNST cells were incubated on ice for 15 minutes with a solution containing 0.025% Crystal Violet and 20% methanol. After three washes with mQ H_2O, Crystal Violet was solubilized in 100% methanol under shaking for at least half an hour. The absorbance related to each cell sample was then read at 595 nm taking advantage of a TECAN plate reader.

4.4. Transwell assays

The Transwell assay was used to assess the migration potential of SCR, TRAP1 KO and COL VI KO sMPNST cells grown in either high or low glutamine (2 mM and 0.6 mM, respectively). As shown in fig. 4.1, Transwell inserts with polyester (PET) membranes and 8.0 μm pores (cell QART®, Cat. No. 9328012) were inserted into the wells of a culture plate in order to create two different compartments, hereafter referred to as upper chamber and bottom chamber. In order to boost cell migration, a chemical gradient was generated between the two compartments using SILAC medium supplemented with 10% dFBS in the lower chamber and SILAC medium supplemented with 0.05% dFBS in the upper chamber.

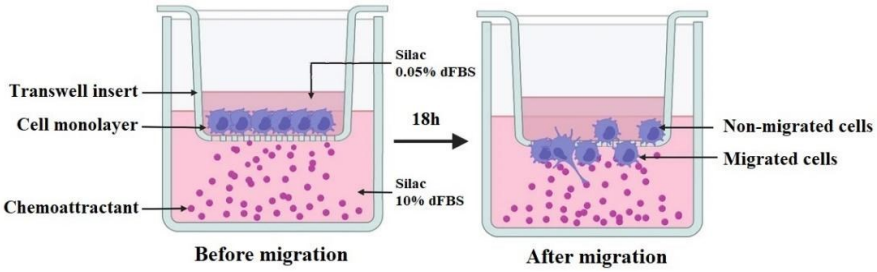

Figure 4.1. Transwell assay. *This Figure shows the two different chambers of a 24-well plate which are separated by a PET membrane. Cells migrate from the upper to the bottom chamber thanks to a chemotactic gradient. Image adapted from Justus et al., 2023.*

500 µl SILAC DMEM Flex Media supplemented with either 2 mM or 0.6 mM Gln, 0.06 mM Arg, and 10% dFBS were added to each bottom chamber in the 24-well plate, and Transwell inserts were placed in. Hence, $3x10^4$ cells were resuspended in 200 µl of SILAC DMEM Flex Media supplemented with either 2 mM or 0.6 mM Gln, 0.06 mM Arg, and 0.05% dFBS and seeded on top of the porous membrane of the upper chamber. After 18-hour incubation the Transwell inserts were stained with RAL Diff-Quik™ kit (RAL DIAGNOSTICS, Cat. No. 7205550000) in order to assess the migration of sMPNST cells from the upper to the bottom chamber. Representative images were taken with a LEICA S9i microscope, and the migration area was analysed with ImageJ software.

4.5. Spheroid culture

$3x10^3$ sMPNST cells were resuspended in 100 µL SILAC DMEM Flex Media supplemented with either 2 mM or 0.6 mM Gln, 0.06 mM Arg, and 1% dFBS, and seeded in each well of CellCarrier Spheroid ULA 96-well Microplate. The plate was then centrifuged at 300*g* for 3 minutes to boost cell aggregation and the formation of 3D spheroid cultures and incubated at 37°C. After 72 hours, 60 µl medium were removed from each well and replaced by an equal volume of matrix solution. This step was quickly performed on ice to avoid matrix polymerization and promote the complete embedding of the spheroid. The plate was hence incubated for a few hours at 37°C to let the matrix polymerize and then, 100 µl SILAC DMEM Flex Media supplemented with either 2 mM or 0.6 mM Gln, 0.06 mM Arg, and 1% dFBS, were added to each well. Spheroids were monitored for 3 days to follow the cancer cell invasion through the matrix. Representative images from each cell line (SCR, TRAP1 KO and COL VI KO sMPNST cells) were taken with a Leica ICC50 HD microscope. The invasion area was analysed with ImageJ software.

4.5.1. Matrix optimization

The "gold-standard" matrix used to test cell invasion is the Matrigel preparation, a mixture of extracellular matrix proteins and growth factors deriving from aggressive sarcomas. Nevertheless, depending on the preparation, Matrigel

solutions may contain COL VI, even if in a small amount. In light of this, in the framework of my thesis, I have optimized different matrices to unequivocally test the contribution of COL VI to sMPNST invasion in both conditions of high and low Gln availability. Hereafter, I report their formulations:

- 0.1% and 0.5% low melting agarose
- 0.1% and 0.5% low melting agarose + 0.048 µg/µl laminin
- 0.1% and 0.5% low melting agarose + 0.1 µg/µl fibronectin
- 0.1% and 0.5% low melting agarose + 0.048 µg/µl laminin + 0.1 µg/µl fibronectin
- 0.1% and 0.5% low melting agarose + 1% Matrigel
- Type-I Collagen
- Type-I Collagen diluted 1:1, 1:10 and 1:100 in 0.1% low melting agarose
- 3 mg/ml Laminin
- 1.5 mg/ml Laminin
- 0.055 mg/ml type-I Collagen, 5.5 mg/ml laminin and 0.073 mg/ml fibronectin (type-I Collagen was previously neutralized with 1M NaOH)
- 1.75 mg/ml type-I Collagen, 3.5 mg/ml laminin and 0.047 mg/ml fibronectin (type-I Collagen was previously neutralized with 1M NaOH).

4.6. Whole-mount immunofluorescence on spheroids

After monitoring invasion across matrix for 4 days, spheroids were stained with several dyes to detect cell nuclei (DAPI) and actin filaments in the cytoskeleton (phalloidin). In particular, spheroids were washed with 1X PBS and then incubated with 4% paraformaldehyde (Electron Microscopy Sciences, Cat.No. 15710) for 1h at room temperature. Next, spheroids were washed with PBS three times for 10 minutes. Hence they were permeabilized with 0.1% Triton X-100 (Sigma, Cat. No. 9036195) for half an hour at room temperature and washed three more times with 1X PBS for 10 minutes. Finally, spheroids were stained with DAPI (Sigma, Cat. No. D95425MG) and phalloidin (Sigma, Cat.No. P1951) in PBS overnight at 4°C. Representative images were taken with the Stellaris 8 Leica confocal microscope.

4.7. Statistical analysis

Data were analysed with GraphPad software, performing two-way analysis of variance (ANOVA) and Tukey's multiple comparisons test.

5. Results

5.1. Glutamine availability affects sMPNST cell proliferation

Cancer cells increase the uptake of several nutrients and rewire their metabolic routes to produce building blocks for biosynthetic purposes and to cope with an uncontrolled growth and a high proliferation rate (Phan et al., 2014). Among other organic substrates, cancer cells strictly depend on Gln, a versatile molecule which fuels several anabolic pathways occurring in mitochondria (Cruzat et al., 2018). Moreover, recent evidence suggests a role for Gln metabolism in the production of collagens and of the ECM via proline biosynthesis (Li et al., 2017). As a first step, in the framework of my thesis project, I tested whether Gln availability could affect proliferation of SCR, TRAP1 KO and COL VI KO sMPNST cells. As described before (see Materials and Methods), sMPNST cell proliferation was monitored on a daily basis up to 5 days by carrying out the Crystal Violet assay. As shown in fig 5.1 and fig 5.2, all the sMPNST cell lines included in these experiments grew in a medium supplemented with a low amount of Gln (0.6 mM Gln) show slower proliferation rates, if compared to cells grown in high Gln (2 mM Gln). Although statistical tests have highlighted no major differences in the proliferation rates among the three different cell genotypes, I have observed a slightly higher proliferation rate for TRAP1 KO sMPNST cells when grown in high Gln, while COL VI KO cells tend to proliferate slower in both high and low Gln conditions. These trends become more evident especially at late time points (96h).

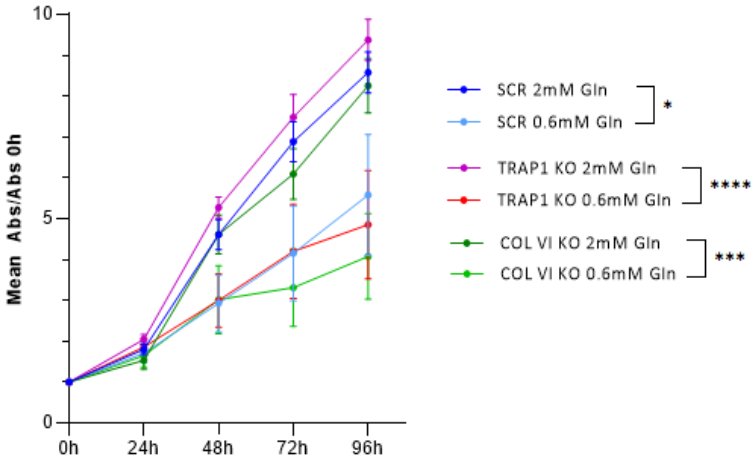

Figure 5.1. Proliferation curves of SCR, TRAP1 KO and COL VI KO sMPNST cells grown in high and low Gln (2 mM and 0.6 mM, respectively). *Proliferation data related to each cell line are shown as the mean absorbance of the Crystal Violet measured every 24 hours and normalized on the absorbance recorded at the 0h time. Measurements were repeated on four biological replicates (n=4). For each experiment four technical replicates/genotype were included. Error bars are shown as ±S.E.M. Statistically analyses were performed by running the Two-way ANOVA test with GraphPad software (*p < 0.05, ** < 0.01, *** < 0.001 and **** < 0.0001).*

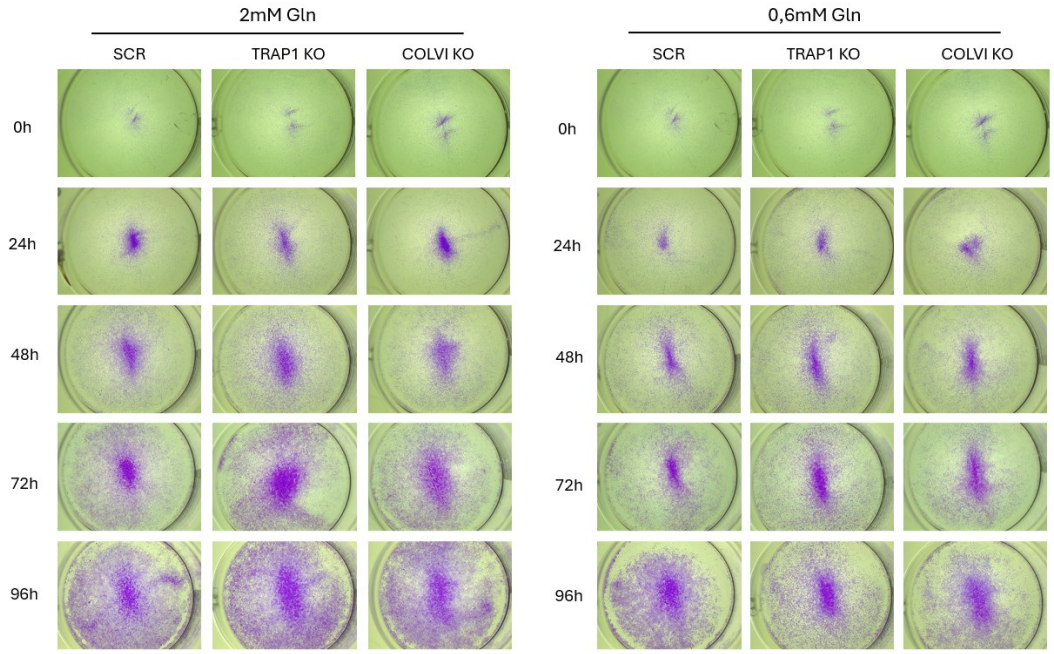

Figure 5.2. Representative images of proliferating cells stained with the Crystal Violet at different time points.

5.2. Effects of TRAP1 and COL VI on the migration of sMPNST cells

ECM remodelling is a leading process in tumour development (Socovich and Naba, 2019). Cancer cells continuously degrade and synthesise new collagen molecules in order to generate local paths that promote their invasion and migration, and to create physical scaffolds that favour cell movements. I have tested the importance of TRAP1 and COL VI for sMPNST cells by performing the Transwell assays. As for the proliferation tests, these *in vitro* experiments were also carried out by growing cells in low Gln conditions, in order to mimic its physiological and extracellular levels, and to assess Gln contribution to cell migration. The Transwell assay takes advantage of membranous inserts to generate two compartments that are known as top and bottom chamber. Hence, I have measured cancer cell transition across such porous supports to assess their migration potential.

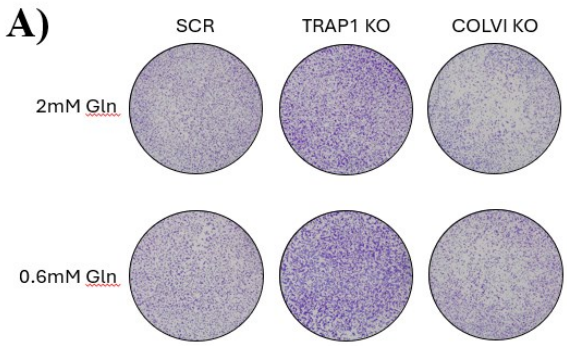

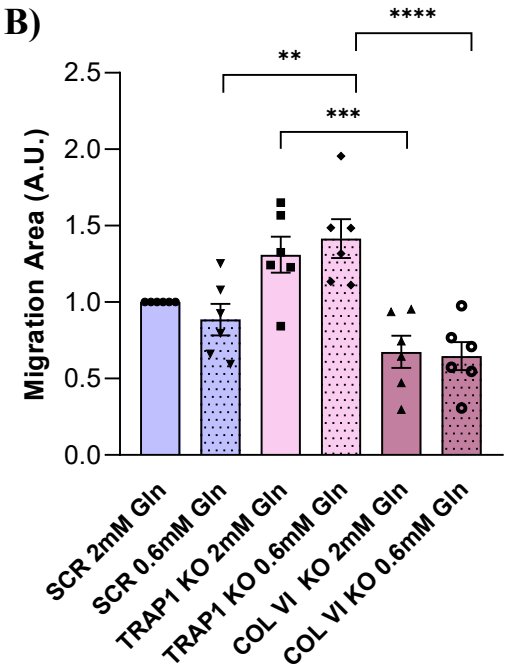

Figure 5.3. A) Representative images of sMPNST cells following migration across Transwell inserts and cytological staining. B) Migration area (in arbitrary units) of SCR, TRAP1 KO and COL VI KO sMPNST cells measured in both high and low Gln (2 mM and 0.6 mM, respectively). *Measurements were repeated on six biological replicates, and for each experiment 3 technical replicates/genotype were included. Data are reported as mean±S.E.M and were analysed with GraphPad software by running the Two-way ANOVA test (*$p < 0.05$, ** < 0.01, *** < 0.001 and **** < 0.0001).

As shown in Fig. 5.3, sMPNST cells lacking COL VI migrate less if compared to SCR cells, while TRAP1 KO cells seem to have a higher migration potential than SCR cells. Moreover, unlike proliferation assay, glutamine availability does not affect sMPNST cell migration.

5.3. Spheroids culture

Among other pro-tumorigenic roles, COL VI has been shown to have important functions in promoting cancer cell invasion (Wishart et al., 2020). To test the importance of COL VI for sMPNST cell invasive properties, I carried out the branching morphogenesis assay. In this assay, cells are grown within round bottom wells where they form three-dimensional (3D) cultures named spheroids embedded in biological matrices that mimic the extracellular mesh. Cell invasiveness is then monitored by measuring the area covered by branches originating from the spheroids and that penetrate across the matrix. Thanks to their 3D architecture, these *in vitro* platforms highly resemble the heterogeneous organisation of solid tumours, with outer layers consisting of proliferating cells and having direct access to nutrients, and a hypoxic inner core that can become necrotic. The invasive potential of sMPNST cells lacking COL VI has been compared with that of SCR and TRAP1 KO cells.

5.3.1. sMPNST cells can grow as spheroids

I first tested the capacity of sMPNST cells to grow as a 3D culture in round bottom microplates coated with ultra-low attachment surface, and in the presence of a low amount of dFBS. Spheroid formation was tested in both high and low Gln conditions. As shown in Fig 5.4, all the cell types used in this project were able to grow as spheroids. No major morphological differences were observed between low and high Gln culture preparations.

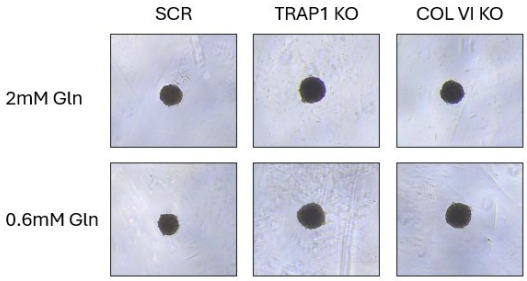

Figure 5.4. Representative images of sMPNST spheroids at three days after seeding.

5.3.2. Matrix optimization for invasiveness studies

As a second step, I tested the ability of sMPNST spheroids to invade after embedding in a biological matrix. As mentioned before (see Materials and Methods), the "gold-standard" matrix used to test cell invasion is Matrigel. I have found that sMPNST spheroids were able to invade when embedded in Matrigel and, in particular, spheroids cultured in 2mM Gln showed a higher invasive potential if compared to spheroids cultured in 0.6mM Gln (Fig. 5.5). However, Matrigel may contain COL VI, even if in a small amount.

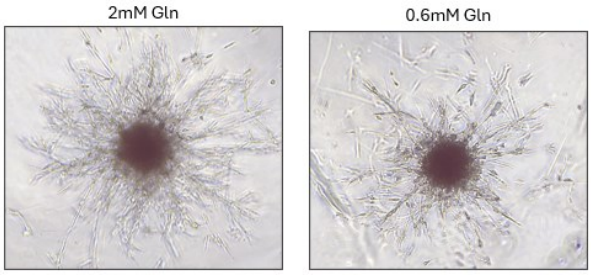

Figure 5.5. Representative images of SCR sMPNST cells invading through Matrigel.

To unequivocally test the contribution of COL VI to sMPNST invasion, I have therefore optimised different matrices. Matrix optimization experiments were performed only with SCR sMPNST cells in both high and low Gln. I first took advantage of low melting agarose (hereafter referred to as LM agar), an inexpensive, easy to prepare polysaccharide with excellent gelling features, optical features (for example optimal clarity in gel phase) and adaptable mechanical and diffusion properties. Several research groups have already used agarose as a

substrate to test cancer spheroid invasiveness (Chong et al., 2024; Quarta et al., 2021). Agarose was tested at different concentrations, and was supplemented with ECM proteins (namely laminin and fibronectin, two major components of the biological ECM) that are widely used in cell culture procedures. Hereafter, I report the formulations of all the different agarose-based matrices I have tested:

- 0.1% and 0.5% LM agar (Matrix 1 and 2, respectively);
- 0.1% and 0.5% LM agar + 0.1 µg/µl fibronectin (Matrix 3 and 4, respectively);
- 0.1% and 0.5% LM agar + 0.048 µg/µl laminin (Matrix 5 and 6, respectively);
- 0.1% and 0.5% LM agar + 0.048 µg/µl laminin + 0.1 µg/µl fibronectin (Matrix 7 and 8, respectively);
- 0.1% and 0.5% LM agar + 1% Matrigel (Matrix 9 and 10 respectively).

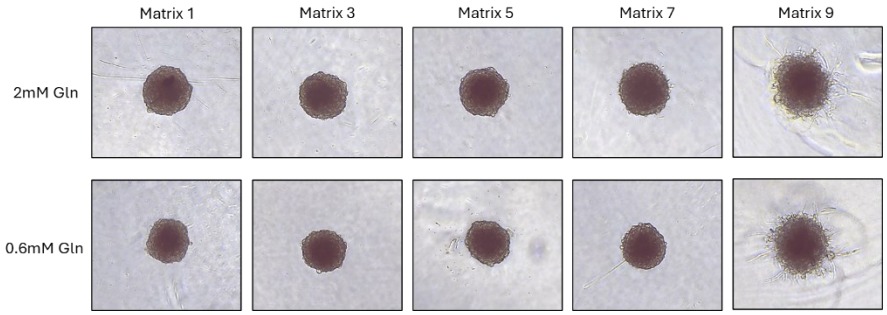

Figure 5.6. Representative images of SCR sMPNST spheroids cultured in 0.1% LM agarose, supplemented with different proteins from the ECM. *Pictures were taken at 3 days after matrix addition.*

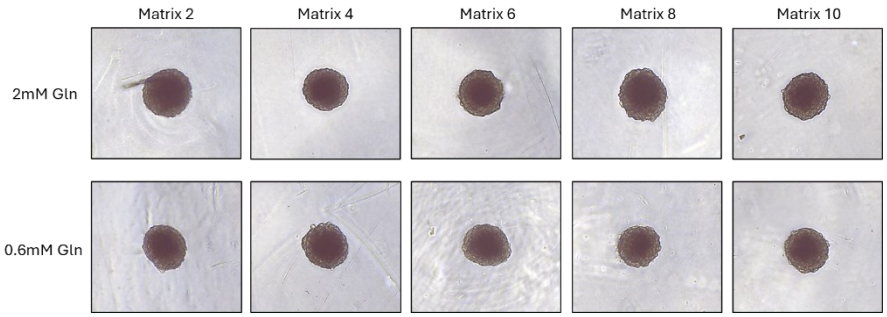

Figure 5.7. Representative images of SCR sMPNST spheroids cultured in 0.5% LM agarose, supplemented with different proteins from the ECM. *Pictures were taken at 3 days after matrix addition.*

As shown in Fig. 5.6 and 5.7, none of the aforementioned conditions promoted sMPNST cell invasion, and no major differences were ascribed to Gln availability. Nevertheless, spheroids embedded in Matrix 3 (0.1% agarose supplemented with

1% Matrigel) formed several invading branches, even though shorter and thinner in shape if compared to those that form in Matrigel alone (see figure 5.5). This result suggested that i) at a higher concentration (0.5%) agarose forms a highly dense mesh that could hamper the passage of cell branches and their invasion; ii) Matrigel components are required for sMPNST cell invasion.

In light of these results, I optimized the preparation of additional matrices including the major Matrigel protein components. As shown in the product datasheet (https://ecatalog.corning.com/life-sciences/b2c/US/en/Surfaces/Extracellular-Matrices-ECMs/Corning%C2%AE-Matrigel%C2%AE-Matrix/p/356231), the main proteins found in Matrigel preparation are:

- Collagens (with collagen IV as the most abundant, followed by others such as COL VI, collagen I that are present in lower amounts);
- Laminins, which bind to integrin receptors located on the cell membrane, hence anchoring cells to the ECM;
- Additional proteins, which are included in small amounts (*e.g.*: fibronectin, entactin, etc.)

Collagen I (COL I) solution was already available in my lab, hence I first prepared and tested several COL I-based matrices. Hereafter, I report their formulations:

- COL I
- COL I/0.1% LM agar in a 1:1 ratio
- COL I/0.1% LM agar in a 1:10 ratio
- COL I/0.1% LM agar in a 1:100 ratio

However, as shown in Fig. 5.8, none of the COL I-based matrices allowed cancer cell invasion.

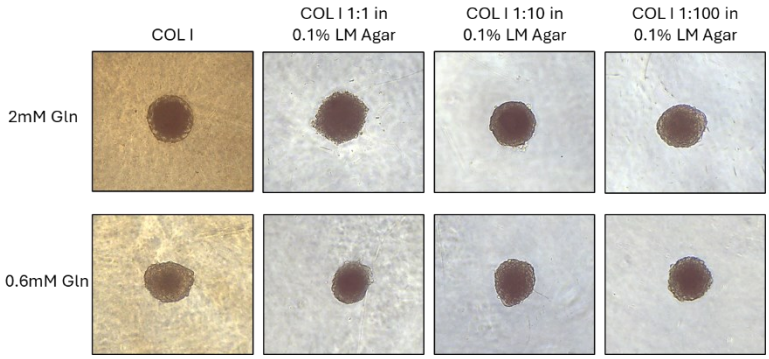

Figure 5.8. Representative images of SCR sMPNST spheroids cultured in different matrix formulations with COL I and LM Agar. *Pictures were taken at 3 days after matrix addition.*

As a next step, I prepared and tested several laminin-based matrices. Laminins are the principal components of Matrigel and are involved in many stages of cancer progression. When used at high concentrations, laminin preparations undergo polymerization and form mesh structures that are suitable for invasion tests. In my experiments, I prepared matrices including either 3 mg/ml or 1.5 mg/ml laminin. As shown in figure 5.9, I have observed the formation of several branches from the cancer cells spheroids embedded in laminin. However, these protrusions were much shorter if compared to those that form in Matrigel (see above, figure 5.5).

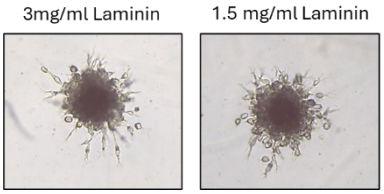

Figure 5.9. Representative images of SCR sMPNST spheroids embedded in matrices including different concentrations of laminin. *Images were taken 3 days after matrix addition.*

Altogether, these results suggested that cancer cell invasion not only depended on the presence of specific components in the microenvironment, but also on their relative abundances and ratios. Hence, I set up two additional matrices by mixing COL I, laminin and fibronectin in ratios similar to those found in Matrigel preparations. Hereafter, I refer to these two matrices as "Matrix A" and "Matrix B"; their formulation is reported below: 1.75 mg/ml COL I, 3.5 mg/ml laminin, 0.047 mg/ml fibronectin (Matrix A); 0.055 mg/ml COL I, 5.5 mg/ml laminin, 0.073 mg/ml fibronectin (Matrix B).

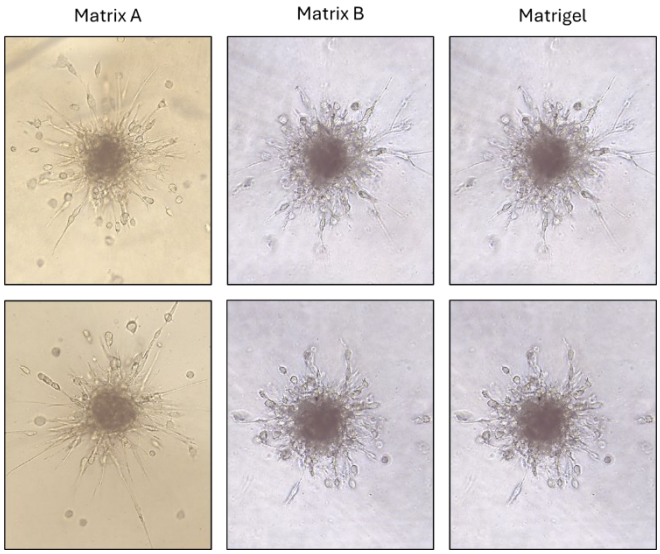

Figure 5.10. Representative images of SCR sMPNST spheroids cultured in two matrices including COL I, laminin and fibronectin in different ratios. *Images of spheroids embedded in Matrigel are included for comparison. Pictures were taken at 3 days after matrix addition.*

As shown in Fig. 5.10, I observed invasion of spheroids embedded in both Matrix A and in Matrix B. However, spheroids embedded in Matrix A (which contains a higher quantity of COL I: 1.75mg/ml) formed longer branches and thus showed a higher invasive potential if compared to spheroids embedded in Matrix B.

5.3.3. Branching morphogenesis experiments

The optimization of a COL VI-free matrix required a longer time than expected. For this reason, during my internship I performed only one branching morphogenesis experiment (n = 1) by taking advantage of the newly-optimised Matrix A. The invasion potential of SCR, TRAP1 KO and COL VI KO cells was tested by culturing them only in high Gln (2 mM). As shown in figure 5.11, COL VI KO sMPNST cells seem to have a lower invasive potential when compared to SCR and TRAP1 KO cells. No major differences in the area covered by cancer cell branches were observed between SCR cells and TRAP1 KO cells. Further experiments will be needed to obtain statistically significant, sound data.

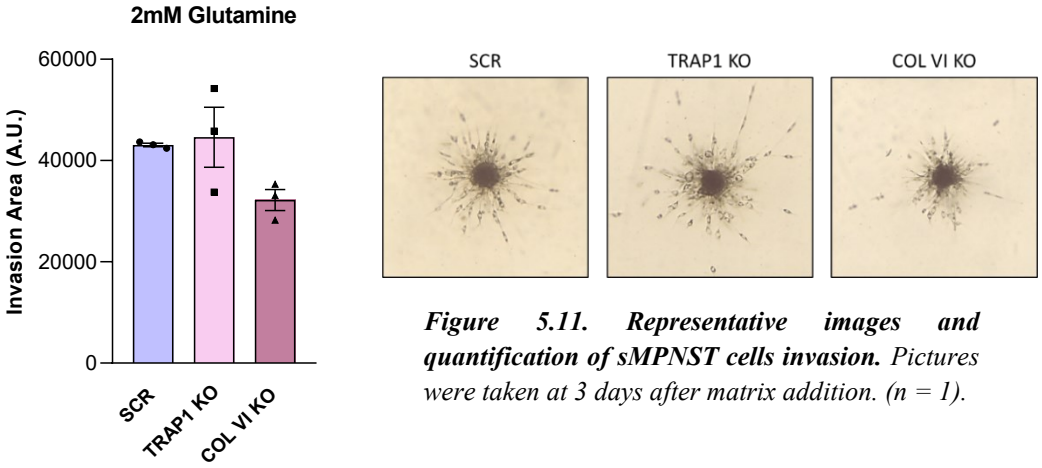

Figure 5.11. Representative images and quantification of sMPNST cells invasion. *Pictures were taken at 3 days after matrix addition. (n = 1).*

5.3.4. Whole-mount immunofluorescence on spheroids

In order to obtain a more precise assessment of the area covered by the branches which originate from spheroids, I started the optimization of whole-mount immunostaining. The use of antibodies conjugated to fluorophores that recognize specific cell components allows a fine reconstruction by confocal microscopy inspections of the whole spheroid structure by 3D projections. As a preliminary experiment, I took advantage of DAPI, which stains nuclei, and of phalloidin, which labels actin molecules in the cytoskeleton.

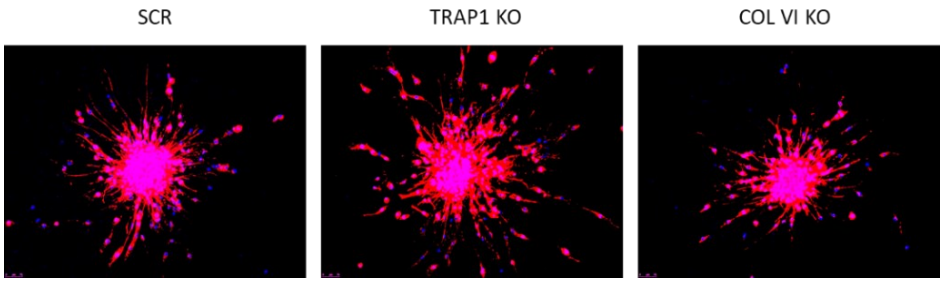

Figure 5.12. Representative images of SCR, TRAP1 KO and COL VI KO sMPNST spheroids stained with DAPI and phalloidin. *Pictures were taken at 4 days after matrix addition with magnification 10X.*

As shown in figure 5.12, both fluorescent dyes showed a target-specific signal, and penetrated across the different layers of the cancer cell spheroids, reaching their inner core. 3D quantification of spheroid invasion is still ongoing. I plan to complete this analysis in the next months, during a research experience as a predoctoral fellow. In the next months, I will also extend whole-mount spheroid analysis by immunostaining with the use of invasion markers.

6. Discussion

My thesis project is part of a study aimed at assessing the contribution of amino acid metabolism to the ECM deposition involved in the development of malignant peripheral nerve sheath tumors (MPNSTs), aggressive sarcomas for which no cure currently exists, as well as at dissecting the regulatory role played by mitochondrial metabolism in this process. Recent evidences suggest that, beside promoting the biosynthesis of building blocks which are required for cancer cell growth and proliferation, the rewiring of amino acid metabolism is important to support collagen biosynthesis and thus in the assembly of the ECM. Preliminary *in vitro* experiments carried out with sMPNST cells in the lab leaded by Prof. Andrea Rasola have shown that: i) levels of COL VI depend on Gln availability; ii) COL VI protein levels are higher in sMPNST expressing TRAP1 if compared to those lacking TRAP1 expression (see Fig. 2.10). Therefore, during my internship, I investigated both Gln and COL VI contribution to sMPNST cell tumorigenicity. To this aim, I used COL VI KO sMPNST cells, which have recently been generated by taking advantage of the CRISPR/CAS9 genome editing technology (see Fig. 2.11), to run several tumorigenic assays at different Gln concentrations.

Following malignant transformation, neoplastic cells increase their rate of proliferation. To adapt to this new phenotype, cancer cells increase the uptake of several nutrients and rewire their metabolic pathways. Among other nutrients, cancer cells significantly increase the uptake and rewire the metabolism of Gln, which fuels a variety of anabolic pathways (Cruzat et al., 2018). By using the Crystal Violet assay, a well-established protocol to assess cell proliferation, I observed a Gln-dependent effect on cell growth, with sMPNST cells growing faster when cultured with extra-physiological concentrations of Gln (2mM). These results clearly indicate that sMPNST cells are characterized by a strong Gln addiction, and that therapeutic strategies aimed at targeting Gln metabolism could limit the growth of MPNSTs. In addition, COL VI KO cells show slower proliferation rates if compared to SCR and TRAP1 KO cells in both Gln conditions. Accordingly, COL VI has been shown to serve as both pro-survival and antiapoptotic factor (Cescon et al., 2016: Cheng et al., 2011). On the contrary, TRAP1 KO cells have shown a slightly higher proliferation rates if compared to SCR and COL VI KO cells when grown in high Gln conditions. This observation could be in contrast with the pro-tumorigenic role ascribed to TRAP1 which is reported in many investigations (Sciacovelli et al., 2013). Nevertheless, TRAP1 is a molecular chaperone and it interacts with a variety of partners, whose identity could change depending on the cell type. As a corollary, TRAP1 could exert either a pro-tumorigenic or a protective role depending on the tumour type.

To have a more complete view of the importance of Gln and COL VI for the tumorigenicity of sMPNST cells, I set up *in vitro* migration and invasion assays. I observed that sMPNST cells lacking COL VI are characterized by a lower

migration potential if compared to SCR and TRAP1 KO cells. This result is in line with previous studies reporting that COL VI promotes cancer cell adhesion and spreading, thus enhancing formation of tumor metastasis (Han et al., 1995). The mitochondrial chaperone TRAP1 is known to stabilise HIF-1α, a transcription factor which enhances the expression of several genes involved in cell invasion (Semenza et al., 2013). In addition, TRAP1 seems to be involved in the regulation of COL VI levels, as higher COL VI levels were observed in sMPNST cells expressing TRAP1 if compared to TRAP1 KO sMPNST cells (Fig. 2.10). Nevertheless, in my experimental setting, TRAP1 KO cells migrated to a higher extent if compared to COL VI KO cells. A possible explanation for this phenomenon could imply the development of adaptation mechanisms by cancer cells to overcome the lack of TRAP1 expression. In addition, cancer cells are characterized by an extremely high genome instability. Mutations in signalling pathways controlling invasive processes could have occurred in TRAP1 KO cells. To exclude the aforementioned possibilities, it could be useful to repeat the Transwell assay with sMPNST cells in which TRAP1 has been ablated in an acute way. In the next months, I will plan the generation of new TRAP1 KO sMPNST cells.

No major differences in cancer cell migration were ascribed to Gln availability. The influence on proliferation rate and the lack of effect on migration properties of sMPNST cells suggest that Gln could play an important role especially in the first steps of the tumorigenic process, leading to a rapid growth of the primary tumor mass, while COL VI would mainly influence later stages of the disease.

To test sMPNST cell invasion, I optimized the compositions of several matrices. The goal was to obtain a formulation free in COL VI, but still able to polymerize and generate a mesh through which cancer cells could move. In matrices composed of low melting agarose alone or in combination with several proteins of the ECM (namely laminin, fibronectin and COL I, which are all known to be involved in cancer cell invasion) sMPNST did not form any invasive branch (De Arcangelis et al., 2001; Oikawa et al., 2011; Gopal et al., 2017; Zhong et al., 2021). It is likely that the mechanical pressure which generates in LM agar-based matrices, cannot stimulate sMPNST cell invasion. Indeed, the type of mechanical force which generates at edge between cell compartment and the extracellular space largely depend on the kind of molecules found in the ECM but also on their respective amounts, as well as on the types of interactions that establish among them. In matrices composed of COL I, laminin and fibronectin in ratios similar to those found in Matrigel preparation, sMPNST cells were able to generate long invading protrusions, generating from the spheroid masses. These results suggest that the invasive potential of cancer cells depends not only on the presence of specific molecules in the extracellular space, but also on their relative proportions. Since the optimization of a matrix suitable to test the invasiveness of sMPNST cells took a longer time than expected, I could include in this thesis only one branching

morphogenesis experiment. Although preliminary, the results of this test show a trend similar to that observed in the migration experiments, with COL VI KO cells showing a lower invasive potential if compared to SCR cells, and with TRAP1 KO cells forming longer branches and in a higher number. Further replicates will be needed to consolidate these data. Also in this case, the generation of new mutants could be useful to assess the establishment of any compensatory and pro-tumorigenic mechanism in TRAP1 KO cells.

In order to implement a more accurate analysis of the invasion area, I started the optimization of immunofluorescence protocols on sMPNST spheroids. Pilot experiments performed with DAPI nuclear staining and phalloidin allowed the reconstruction of the whole volume of the invading spheroids by fluorescence confocal microscopy. In this respect, it worth mentioning that invasive branches could consist of both single cancer cells which protrude from the spheroid core and explore the extracellular environment, as well as of chains of multiple cells that move following linear patterns. Accordingly, as shown in figure 5.12, the DAPI nuclear staining allow the detection of several cancer cell nuclei scattered around the main spheroid mass.

Altogether, the experiments included in this thesis indicate that Gln metabolism rewiring in cancer cells promotes MPNST development during all its steps. In particular, in the more advanced phases of the disease, Gln metabolism would favour cancer cell invasion and migration by supporting the formation of an ECM enriched in COL VI molecules. The mitochondrial chaperone TRAP1 would finely coordinate these processes, in order to optimize the biosynthesis of Pro. It is likely that TRAP1 regulates the conversion of Gln into Pro by modulating the activity of several enzymes including GLS1 and ALDH18A1, which have recently been identified as its interacting partners (see figure 2.8). Alternatively, TRAP1 could indirectly affect COL VI production by inhibiting the SDH activity and promoting the activation of HIF1α, which has been shown to regulate the expression of PH4, an enzyme involved in collagen molecule maturation. Together with further tumorigenic and immunofluorescence assays, in the next months, as a predoctoral fellow in the lab leaded by Prof Andrea Rasola, I will dissect the molecular mechanism(s) behind COL VI regulation by TRAP1. A deeper comprehension of the molecular processes contributing to the pathogenesis of MPNST is mandatory to design effective therapeutic approaches and hamper its growth.

7. References

Abramowicz A, Gos M. Neurofibromin in neurofibromatosis type 1 - mutations in NF1gene as a cause of disease. Dev Period Med. 2014 Jul-Sep;18(3):297-306. PMID: 25182393.

Amelio I, Cutruzzolá F, Antonov A, Agostini M, Melino G. Serine and glycine metabolism in cancer. Trends Biochem Sci. 2014 Apr;39(4):191-8. doi: 10.1016/j.tibs.2014.02.004. Epub 2014 Mar 20. PMID: 24657017; PMCID: PMC3989988.

Belhabib I, Zaghdoudi S, Lac C, Bousquet C, Jean C. Extracellular Matrices and Cancer-Associated Fibroblasts: Targets for Cancer Diagnosis and Therapy? Cancers (Basel). 2021 Jul 11;13(14):3466. doi: 10.3390/cancers13143466. PMID: 34298680; PMCID: PMC8303391.

Bonuccelli G, Tsirigos A, Whitaker-Menezes D, Pavlides S, Pestell RG, Chiavarina B, Frank PG, Flomenberg N, Howell A, Martinez-Outschoorn UE, Sotgia F, Lisanti MP. Ketones and lactate "fuel" tumor growth and metastasis: Evidence that epithelial cancer cells use oxidative mitochondrial metabolism. Cell Cycle. 2010 Sep 1;9(17):3506-14. doi: 10.4161/cc.9.17.12731. Epub 2010 Sep 21. PMID: 20818174; PMCID: PMC3047616.

Brohl AS, Kahen E, Yoder SJ, Teer JK, Reed DR. The genomic landscape of malignant peripheral nerve sheath tumors: diverse drivers of Ras pathway activation. Sci Rep. 2017 Nov 8;7(1):14992. doi: 10.1038/s41598-017-15183-1. PMID: 29118384; PMCID: PMC5678116.

Buschmann MD, Grodzinsky AJ. A molecular model of proteoglycan-associated electrostatic forces in cartilage mechanics. J Biomech Eng. 1995 May;117(2):179-92. doi: 10.1115/1.2796000. PMID: 7666655.

Butler EK, Voigt A, Lutz AK, Toegel JP, Gerhardt E, Karsten P, Falkenburger B, Reinartz A, Winklhofer KF, Schulz JB. The mitochondrial chaperone protein TRAP1 mitigates α-Synuclein toxicity. PLoS Genet. 2012 Feb;8(2):e1002488. doi: 10.1371/journal.pgen.1002488. Epub 2012 Feb 2. PMID: 22319455; PMCID: PMC3271059.

Cannino G, Urbani A, Gaspari M, Varano M, Negro A, Filippi A, Ciscato F, Masgras I, Gerle C, Tibaldi E, Brunati AM, Colombo G, Lippe G, Bernardi P, Rasola A. The mitochondrial chaperone TRAP1 regulates F-ATP synthase channel formation. Cell Death Differ. 2022 Dec;29(12):2335-2346. doi: 10.1038/s41418-022-01020-0. Epub 2022 May 25. PMID: 35614131; PMCID: PMC9751095.

Castagnaro S, Gambarotto L, Cescon M, Bonaldo P. Autophagy in the mesh of collagen VI. Matrix Biol. 2021 Jun;100-101:162-172. doi: 10.1016/j.matbio.2020.12.004. Epub 2020 Dec 26. PMID: 33373668.

Cescon M, Chen P, Castagnaro S, Gregorio I, Bonaldo P. Lack of collagen VI promotes neurodegeneration by impairing autophagy and inducing apoptosis during aging. Aging (Albany NY). 2016 May;8(5):1083-101. doi: 10.18632/aging.100924. PMID: 27060109; PMCID: PMC4931855.

Chandra D, Singh KK. Genetic insights into OXPHOS defect and its role in cancer. Biochim Biophys Acta. 2011 Jun;1807(6):620-5. doi: 10.1016/j.bbabio.2010.10.023. Epub 2010 Nov 11. PMID: 21074512; PMCID: PMC4681500.

Cheng IH, Lin YC, Hwang E, Huang HT, Chang WH, Liu YL, Chao CY. Collagen VI protects against neuronal apoptosis elicited by ultraviolet irradiation via an Akt/phosphatidylinositol 3-kinase signaling pathway. Neuroscience. 2011 Jun 2;183:178-88. doi: 10.1016/j.neuroscience.2011.03.057. Epub 2011 Apr 1. PMID: 21459131.

Chong LH, Yip AK, Farm HJ, Mahmoud LN, Zeng Y, Chiam KH. The role of cell-matrix adhesion and cell migration in breast tumor growth and progression. Front Cell Dev Biol. 2024 Feb 5;12:1339251. doi: 10.3389/fcell.2024.1339251. PMID: 38374894; PMCID: PMC10875056.

Cruzat V, Macedo Rogero M, Noel Keane K, Curi R, Newsholme P. Glutamine: Metabolism and Immune Function, Supplementation and Clinical Translation. Nutrients. 2018 Oct 23;10(11):1564. doi: 10.3390/nu10111564. PMID: 30360490; PMCID: PMC6266414.

De Arcangelis A, Lefebvre O, Méchine-Neuville A, Arnold C, Klein A, Rémy L, Kedinger M, Simon-Assmann P. Overexpression of laminin alpha1 chain in colonic cancer cells induces an increase in tumor growth. Int J Cancer. 2001 Oct 1;94(1):44-53. doi: 10.1002/ijc.1444. PMID: 11668477.

DeClue JE, Cohen BD, Lowy DR. Identification and characterization of the neurofibromatosis type 1 protein product. Proc Natl Acad Sci U S A. 1991 Nov 15;88(22):9914-8. doi: 10.1073/pnas.88.22.9914. PMID: 1946460; PMCID: PMC52837.

Desgrosellier JS, Cheresh DA. Integrins in cancer: biological implications and therapeutic opportunities. Nat Rev Cancer. 2010 Jan;10(1):9-22. doi: 10.1038/nrc2748. PMID: 20029421; PMCID: PMC4383089.

Duan, Y.; Liu, G.; Sun, Y.; Wu, J.; Xiong, Z.; Jin, T.; Chen, M. Collagen Type VI A5 Gene Variations May Predict the Risk of Lung Cancer Development in Chinese Han Population. Sci. Rep. 2020, 10, 5010.

Evans DG, Howard E, Giblin C, Clancy T, Spencer H, Huson SM, Lalloo F. Birth incidence and prevalence of tumor-prone syndromes: estimates from a UK family genetic register service. Am J Med Genet A. 2010 Feb;152A(2):327-32. doi: 10.1002/ajmg.a.33139. PMID: 20082463.

Friedman JM. Neurofibromatosis 1: clinical manifestations and diagnostic criteria. J Child Neurol. 2002 Aug;17(8):548-54; discussion 571-2, 646-51. doi: 10.1177/088307380201700802. PMID: 12403552.

Gao JY, Song BR, Peng JJ, Lu YM. Correlation between mitochondrial TRAP-1 expression and lymph node metastasis in colorectal cancer. World J Gastroenterol. 2012 Nov 7;18(41):5965-71. doi: 10.3748/wjg.v18.i41.5965. PMID: 23139614; PMCID: PMC3491605.

Gattazzo F, Urciuolo A, Bonaldo P. Extracellular matrix: a dynamic microenvironment for stem cell niche. Biochim Biophys Acta. 2014 Aug;1840(8):2506-19. doi: 10.1016/j.bbagen.2014.01.010. Epub 2014 Jan 10. PMID: 24418517; PMCID: PMC4081568.

Gopal S, Veracini L, Grall D, Butori C, Schaub S, Audebert S, Camoin L, Baudelet E, Radwanska A, Beghelli-de la Forest Divonne S, Violette SM, Weinreb PH, Rekima S, Ilie M, Sudaka A, Hofman P, Van Obberghen-Schilling E. Fibronectin-guided migration of carcinoma collectives. Nat Commun. 2017 Jan 19;8:14105. doi: 10.1038/ncomms14105. PMID: 28102238; PMCID: PMC5253696.

Guo L, Cui C, Zhang K, Wang J, Wang Y, Lu Y, Chen K, Yuan J, Xiao G, Tang B, Sun Y, Wu C. Kindlin-2 links mechano-environment to proline synthesis and tumor growth. Nat Commun. 2019 Feb 19;10(1):845. doi: 10.1038/s41467-019-08772-3. PMID: 30783087; PMCID: PMC6381112.

Guo L, Cui C, Wang J, Yuan J, Yang Q, Zhang P, Su W, Bao R, Ran J, Wu C. PINCH-1 regulates mitochondrial dynamics to promote proline synthesis and tumor growth. Nat Commun. 2020 Oct 1;11(1):4913. doi: 10.1038/s41467-020-18753-6. PMID: 33004813; PMCID: PMC7529891.

Gutmann DH, Ferner RE, Listernick RH, Korf BR, Wolters PL, Johnson KJ. Neurofibromatosis type 1. Nat Rev Dis Primers. 2017 Feb 23;3:17004. doi: 10.1038/nrdp.2017.4. PMID: 28230061.

Halper J, Progress in Heritable Soft Connective Tissue Disease, 2021. https://doi.org/10.1007/978-3-030-80614-9

Han J, Daniel JC. Biosynthesis of type VI collagen by glioblastoma cells and possible function in cell invasion of three-dimensional matrices. Connect Tissue Res. 1995;31(2):161-70. doi: 10.3109/03008209509028404. PMID: 15612332.

Ho, C.-M.; Chang, T.-H.; Yen, T.-L.; Hong, K.-J.; Huang, S.-H. Collagen Type VI Regulates the CDK4/6-p-Rb Signaling Pathway and Promotes Ovarian Cancer Invasiveness, Stemness, and Metastasis. Am. J. Cancer Res. 2021, 11, 668–690.

Iyengar, P.; Espina, V.; Williams, T.W.; Lin, Y.; Berry, D.; Jelicks, L.A.; Lee, H.; Temple, K.; Graves, R.; Pollard, J.; et al. Adipocyte-Derived Collagen VI Affects Early Mammary Tumor Progression In Vivo, Demonstrating a Critical Interaction in the Tumor/Stroma Microenvironment. J. Clin. Investig. 2005, 115, 1163–1176.

Justus, C.R., Marie, M.A., Sanderlin, E.J., Yang, L.V. (2023). Transwell In Vitro Cell Migration and Invasion Assays. In: Friedrich, O., Gilbert, D.F. (eds) Cell Viability Assays. Methods in Molecular Biology, vol 2644. Humana, New York, NY. https://doi.org/10.1007/978-1-0716-3052-5_22

Jabłońska-Trypuć, A., Matejczyk, M., & Rosochacki, S. (2016). Matrix metalloproteinases (MMPs), the main extracellular matrix (ECM) enzymes in collagen degradation, as a target for anticancer drugs. Journal of Enzyme Inhibition and Medicinal Chemistry, 31(sup1), 177–183. https://doi.org/10.3109/14756366.2016.1161620

Jaldin-Fincati JR, Pavarotti M, Frendo-Cumbo S, Bilan PJ, Klip A. Update on GLUT4 Vesicle Traffic: A Cornerstone of Insulin Action. Trends Endocrinol Metab. 2017 Aug;28(8):597-611. doi: 10.1016/j.tem.2017.05.002. Epub 2017 Jun 8. PMID: 28602209.

Kay, E.J., Paterson, K., Riera-Domingo, C. et al. Cancer-associated fibroblasts require proline synthesis by PYCR1 for the deposition of pro-tumorigenic extracellular matrix. Nat Metab 4, 693–710 (2022). https://doi.org/10.1038/s42255-022-00582-0.

Keith B, Johnson RS, Simon MC. HIF1α and HIF2α: sibling rivalry in hypoxic tumour growth and progression. Nat Rev Cancer. 2011 Dec 15;12(1):9-22. doi: 10.1038/nrc3183. PMID: 22169972; PMCID: PMC3401912.

Kluwe L, Friedrich R, Mautner VF. Loss of NF1 allele in Schwann cells but not in fibroblasts derived from an NF1-associated neurofibroma. Genes Chromosomes Cancer. 1999 Mar;24(3):283-5. doi: 10.1002/(sici)1098-2264(199903)24:3<283::aid-gcc15>3.0.co;2-k. PMID: 10451710.

Laycock-van Spyk S, Thomas N, Cooper DN, Upadhyaya M. Neurofibromatosis type 1-associated tumours: their somatic mutational spectrum and pathogenesis.

Hum Genomics. 2011 Oct;5(6):623-90. doi: 10.1186/1479-7364-5-6-623. PMID: 22155606; PMCID: PMC3525246.

Le Q.L., Shipman T., Burns D.K., Parada L.F. Cell of origin and microenvironment contribution for NF1-associated dermal neurofibromas. Cell Stem Cell. 2009; 4:453-463. [Pubmed: 19427294]

Lee W, Teckie S, Wiesner T, Ran L, Prieto Granada CN, Lin M, Zhu S, Cao Z, Liang Y, Sboner A, Tap WD, Fletcher JA, Huberman KH, Qin LX, Viale A, Singer S, Zheng D, Berger MF, Chen Y, Antonescu CR, Chi P. PRC2 is recurrently inactivated through EED or SUZ12 loss in malignant peripheral nerve sheath tumors. Nat Genet. 2014 Nov;46(11):1227-32. doi: 10.1038/ng.3095. Epub 2014 Sep 21. PMID: 25240281; PMCID: PMC4249650.

Li J, Ghazwani M, Liu K, Huang Y, Chang N, Fan J, He F, Li L, Bu S, Xie W, Ma X, Li S. Regulation of hepatic stellate cell proliferation and activation by glutamine metabolism. PLoS One. 2017 Aug 10;12(8):e0182679. doi: 10.1371/journal.pone.0182679. PMID: 28797105; PMCID: PMC5552314.

Mak KM, Mei R. Basement Membrane Type IV Collagen and Laminin: An Overview of Their Biology and Value as Fibrosis Biomarkers of Liver Disease. Anat Rec (Hoboken). 2017 Aug;300(8):1371-1390. doi: 10.1002/ar.23567. Epub 2017 Feb 28. PMID: 28187500.

Masgras I, Sanchez-Martin C, Colombo G, Rasola A. The Chaperone TRAP1 As a Modulator of the Mitochondrial Adaptations in Cancer Cells. Front Oncol. 2017 Mar 29;7:58. doi: 10.3389/fonc.2017.00058. PMID: 28405578; PMCID: PMC5370238.

Montesano Gesualdi N, Chirico G, Pirozzi G, Costantino E, Landriscina M, Esposito F. Tumor necrosis factor-associated protein 1 (TRAP-1) protects cells from oxidative stress and apoptosis. Stress. 2007 Nov;10(4):342-50. doi: 10.1080/10253890701314863. PMID: 17853063.

Naba A. Mechanisms of assembly and remodelling of the extracellular matrix. Nat Rev Mol Cell Biol. 2024 Nov;25(11):865-885. doi: 10.1038/s41580-024-00767-3. Epub 2024 Sep 2. PMID: 39223427.

Oikawa Y, Hansson J, Sasaki T, Rousselle P, Domogatskaya A, Rodin S, Tryggvason K, Patarroyo M. Melanoma cells produce multiple laminin isoforms and strongly migrate on α5 laminin(s) via several integrin receptors. Exp Cell Res. 2011 May 1;317(8):1119-33. doi: 10.1016/j.yexcr.2010.12.019. Epub 2010 Dec 31. PMID: 21195710.

Owusu-Ansah, K.G.; Song, G.; Chen, R.; Edoo, M.I.A.; Li, J.; Chen, B.; Wu, J.; Zhou, L.; Xie, H.; Jiang, D.; et al. COL6A1 Promotes Metastasis and Predicts Poor Prognosis in Patients with Pancreatic Cancer. Int. J. Oncol. 2019, 55, 391–404.

Phan LM, Yeung SC, Lee MH. Cancer metabolic reprogramming: importance, main features, and potentials for precise targeted anti-cancer therapies. Cancer Biol Med. 2014 Mar;11(1):1-19. doi: 10.7497/j.issn.2095-3941.2014.01.001. PMID: 24738035; PMCID: PMC3969803.

Pompili S, Latella G, Gaudio E, Sferra R, Vetuschi A. The Charming World of the Extracellular Matrix: A Dynamic and Protective Network of the Intestinal Wall. Front Med (Lausanne). 2021 Apr 16;8:610189. doi: 10.3389/fmed.2021.610189. PMID: 33937276; PMCID: PMC8085262.

Quarta A, Gallo N, Vergara D, Salvatore L, Nobile C, Ragusa A, Gaballo A. Investigation on the Composition of Agarose-Collagen I Blended Hydrogels as Matrices for the Growth of Spheroids from Breast Cancer Cell Lines. Pharmaceutics. 2021 Jun 26;13(7):963. doi: 10.3390/pharmaceutics13070963. PMID: 34206758; PMCID: PMC8308953.

Rasola A, Neckers L, Picard D. Mitochondrial oxidative phosphorylation TRAP(1)ped in tumor cells. Trends Cell Biol. 2014 Aug;24(8):455-63. doi: 10.1016/j.tcb.2014.03.005. Epub 2014 Apr 11. PMID: 24731398; PMCID: PMC7670877.

Romani P, Valcarcel-Jimenez L, Frezza C, Dupont S. Crosstalk between mechanotransduction and metabolism. Nat Rev Mol Cell Biol. 2021 Jan;22(1):22-38. doi: 10.1038/s41580-020-00306-w. Epub 2020 Nov 13. PMID: 33188273.

Sciacovelli M, Guzzo G, Morello V, Frezza C, Zheng L, Nannini N, Calabrese F, Laudiero G, Esposito F, Landriscina M, Defilippi P, Bernardi P, Rasola A. The mitochondrial chaperone TRAP1 promotes neoplastic growth by inhibiting succinate dehydrogenase. Cell Metab. 2013 Jun 4;17(6):988-999. doi: 10.1016/j.cmet.2013.04.019. PMID: 23747254; PMCID: PMC3677096.

Semenza GL. Cancer-stromal cell interactions mediated by hypoxia-inducible factors promote angiogenesis, lymphangiogenesis, and metastasis. Oncogene. 2013 Aug 29;32(35):4057-63. doi: 10.1038/onc.2012.578. Epub 2012 Dec 10. PMID: 23222717; PMCID: PMC4415159.

Shen Y, Zhang Y, Li W, Chen K, Xiang M, Ma H. Glutamine metabolism: from proliferating cells to cardiomyocytes. Metabolism. 2021 Aug;121:154778. doi: 10.1016/j.metabol.2021.154778. Epub 2021 Apr 24. PMID: 33901502.

Socovich AM, Naba A. The cancer matrisome: From comprehensive characterization to biomarker discovery. Semin Cell Dev Biol. 2019 May;89:157-166. doi: 10.1016/j.semcdb.2018.06.005. Epub 2018 Jul 13. PMID: 29964200.

Takahashi A, Majumdar A, Parameswaran H, Bartolák-Suki E, Suki B. Proteoglycans maintain lung stability in an elastase-treated mouse model of emphysema. Am J Respir Cell Mol Biol. 2014 Jul;51(1):26-33. doi: 10.1165/rcmb.2013-0179OC. PMID: 24450478; PMCID: PMC4091854.

Theocharis AD, Skandalis SS, Gialeli C, Karamanos NK. Extracellular matrix structure. Adv Drug Deliv Rev. 2016 Feb 1;97:4-27. doi: 10.1016/j.addr.2015.11.001. Epub 2015 Nov 10. PMID: 26562801.

Tyagi K, Mandal S, Roy A. Recent advancements in therapeutic targeting of the Warburg effect in refractory ovarian cancer: A promise towards disease remission. Biochim Biophys Acta Rev Cancer. 2021 Aug;1876(1):188563. doi: 10.1016/j.bbcan.2021.188563. Epub 2021 May 7. PMID: 33971276.

Upadhyay A, Bakkalci D, Micalet A, Butler M, Bergin M, Moeendarbary E, Loizidou M, Cheema U. Dense Collagen I as a Biomimetic Material to Track Matrix Remodelling in Renal Carcinomas. ACS Omega. 2024 Sep 28;9(40):41419-41432. doi: 10.1021/acsomega.4c04442. PMID: 39398183; PMCID: PMC11465592.

Uusitalo E, Rantanen M, Kallionpää RA, Pöyhönen M, Leppävirta J, Ylä-Outinen H, Riccardi VM, Pukkala E, Pitkäniemi J, Peltonen S, Peltonen J. Distinctive Cancer Associations in Patients With Neurofibromatosis Type 1. J Clin Oncol. 2016 Jun 10;34(17):1978-86. doi: 10.1200/JCO.2015.65.3576. Epub 2016 Feb 29. PMID: 26926675.

Vander Heiden MG, Cantley LC, Thompson CB. Understanding the Warburg effect: the metabolic requirements of cell proliferation. Science. 2009 May 22;324(5930):1029-33. doi: 10.1126/science.1160809. PMID: 19460998; PMCID: PMC2849637.

Watson KL, Al Sannaa GA, Kivlin CM, Ingram DR, Landers SM, Roland CL, Cormier JN, Hunt KK, Feig BW, Ashleigh Guadagnolo B, Bishop AJ, Wang WL, Slopis JM, McCutcheon IE, Lazar AJ, Torres KE. Patterns of recurrence and survival in sporadic, neurofibromatosis Type 1-associated, and radiation-associated malignant peripheral nerve sheath tumors. J Neurosurg. 2017 Jan;126(1):319-329. doi: 10.3171/2015.12.JNS152443. Epub 2016 Apr 1. PMID: 27035165; PMCID: PMC5045773.

Wishart AL, Conner SJ, Guarin JR, Fatherree JP, Peng Y, McGinn RA, Crews R, Naber SP, Hunter M, Greenberg AS, Oudin MJ. Decellularized extracellular matrix scaffolds identify full-length collagen VI as a driver of breast cancer cell invasion

in obesity and metastasis. Sci Adv. 2020 Oct 21;6(43):eabc3175. doi: 10.1126/sciadv.abc3175. PMID: 33087348; PMCID: PMC7577726.

Yoshida S, Tsutsumi S, Muhlebach G, Sourbier C, Lee MJ, Lee S, Vartholomaiou E, Tatokoro M, Beebe K, Miyajima N, Mohney RP, Chen Y, Hasumi H, Xu W, Fukushima H, Nakamura K, Koga F, Kihara K, Trepel J, Picard D, Neckers L. Molecular chaperone TRAP1 regulates a metabolic switch between mitochondrial respiration and aerobic glycolysis. Proc Natl Acad Sci U S A. 2013 Apr 23;110(17):E1604-12. doi: 10.1073/pnas.1220659110. Epub 2013 Apr 5. PMID: 23564345; PMCID: PMC3637790.

You WK, Bonaldo P, Stallcup WB. Collagen VI ablation retards brain tumor progression due to deficits in assembly of the vascular basal lamina. Am J Pathol. 2012 Mar;180(3):1145-1158. doi: 10.1016/j.ajpath.2011.11.006. Epub 2011 Dec 23. PMID: 22200614; PMCID: PMC3349878.

Zhong, C., Tao, B., Tang, F., Yang, X., Peng, T., You, J., Xia, K., Xia, X., Chen, L., Peng, L. (2021). Remodeling cancer stemness by collagen/fibronectin via the AKT and CDC42 signaling pathway crosstalk in glioma. Theranostics, 11(4), 1991-2005. https://doi.org/10.7150/thno.50613.